THE GEOLOGICAL SOCIETY OF AMERICA®

Pinnacle features at the base of isolated carbonate buildups marking point sources of fluid offshore Northwest Australia

James Van Tuyl†, Tiago M. Alves, and Lesley Cherns
3D Seismic Laboratory, School of Earth and Ocean Sciences, Cardiff University, Main Building, Park Place, CF10 3AT Cardiff, UK

ABSTRACT

We investigated pinnacle features at the base of late Oligocene–Miocene isolated carbonate buildups using three-dimensional seismic and borehole data from the Browse Basin, Northwest Australia. Brightened seismic reflections, dim spots, and other evidence of fluid accumulation occur below most pinnacle features. An important observation is that all pinnacles generated topography on successive late Oligocene–Miocene paleo-seafloors, therefore forming preferential zones for the settlement of reef-building organisms by raising the paleo-seafloor into the photic zone. Their height ranges from 31 m to 174 m, for a volume varying from 33 km^3 to 11,105 km^3. Most of the pinnacles, however, are less than 2000 km^3 in volume and present heights of 61–80 m. As a result of this work, pinnacles are explained as the first patch reefs formed in association with mud volcanoes or methanogenic carbonates, and they are considered as precluding the growth of the larger isolated carbonate buildups. We postulate that pinnacle features above fluid-flow conduits demonstrate a valid seep-reef relationship, and we propose them to be refined diagnostic features for understanding fluid flow through geological time.

INTRODUCTION

Carbonate strata dominate the Miocene stratigraphy of the Browse Basin, Northwest Australia (Rosleff-Soerensen et al., 2012), and deposition on other equatorial margins (Brouwer and Schwander, 1987; Eberli and Ginsburg, 1987; Grötsch and Mercadier, 1999; Wilson et al., 2000; Pomar, 2001; Fournier et al., 2005). Significantly, the Browse Basin records a change from a carbonate ramp to a rimmed platform during the Cenozoic, with regional data documenting the contiguous growth of carbonate buildups in the shallowest parts of the North West Shelf after the early Oligocene (Rosleff-Soerensen et al., 2012; Belde et al., 2017; Rankey, 2017). To understand what controls carbonate growth on equatorial margins, it is important to explain the onset of isolated carbonate buildup growth in the Browse Basin, and in similar carbonate sequences in the Browse Basin.

Locally, Howarth and Alves (2016) mapped clustered fluid-flow features above late Oligocene–Miocene karst systems and within isolated carbonate buildups. These fluid-flow features were interpreted as being associated with a salt diapir at depth, despite: (1) the absence of thick evaporites in great parts of the Browse Basin, and (2) the presence of the shallow-water Seringapatam Reef in the area interpreted by Howarth and Alves (2016). While the latter authors discussed fluid flow within (and above) the larger isolated carbonate buildups, they did not address the potential significance of migrating fluids on isolated carbonate buildup initiation and growth. Hence, there is still no complete understanding of what controlled the distribution of isolated carbonate buildups in the Browse Basin, and the role migrating fluids may have played during buildup evolution.

In this paper, we document for the first time the relationship between fluid flow and the growth of late Oligocene–Miocene isolated carbonate buildups in the Browse Basin through the interpretation of the Poseidon three-dimensional (3-D) seismic volume. This was done regardless of the presence of the Seringapatam Reef in the study area, as it forms a prominent near-surface carbonate platform that is distinct from the pinnacle features documented in this paper. Therefore, we addressed the following research questions:

(1) What is the origin of fluids and what structures controlled fluid flow in the Browse Basin?

(2) What do pinnacle features observed at the base of isolated carbonate buildups reflect in terms of geological processes?

(3) Was there an active seep-reef relationship in the Browse Basin during the late Oligocene and Miocene?

GEOLOGICAL SETTING

Mesozoic–Cenozoic Evolution of the Browse Basin

The Browse Basin is an offshore sedimentary basin on Australia's North West Shelf, a northeast-striking passive continental margin developed from the Late Jurassic to the present day (Fig. 1; Stephenson and Cadman, 1994; Rosleff-Soerensen et al., 2012, 2016). Located on the southeast edge of the Timor Sea, the Browse Basin exhibits a margin-parallel, landward-dipping half-graben geometry (Fig. 2; Struckmeyer et al., 1998; Rosleff-Soerensen et al., 2012).

Jurassic continental rifting between Greater India and Western Australia (Veevers and Cotteril, 1978; Langhi and Borel, 2008; Rosleff -Soerensen et al., 2012, 2016) generated northeast-trending structures on the North West Shelf, including in the Yampi, Leveque, Caswell, and Barcoo subbasins (Fig. 1; Longley et al., 2002; Langhi and Borel, 2008; Rosleff-Soerensen et al., 2012, 2016; Howarth and Alves, 2016). Early Cretaceous subsidence and the deposition of a passive-margin sequence buried the rift-related topography (Fig. 2; Stephenson and Cadman, 1994; Struckmeyer et al., 1998; Langhi and Borel, 2008; Rosleff-Soerensen et al., 2012).

Seafloor spreading in the Indian and Southern Oceans caused northward migration of Australia from ~40°S in the Eocene–Oligocene to ~20°S at present (Apthorpe, 1988; McGowran et al., 2004; Rosleff-Soerensen et al., 2012). In particular, late Oligocene–early Miocene collision between the Pacific and Australasian plates promoted counterclockwise rotation of the Australian continent (Veevers and Powell, 1984). This rotation generated subsidence and shallow extensional faulting in the outer North West Shelf (Stephenson and Cadman, 1994). Fault reactivation (Harrowfield and Keep, 2005; Rosleff-Soerensen et al., 2012) and moderate tectonic inversion in the Browse Basin (Keep et al., 2000).

The Cenozoic oceanography of the North West Shelf was closely controlled by the Indonesian Throughflow (Fig. 1; McGowran et al.,

†vantuylj@cardiff.ac.uk

GSA Bulletin; https://doi.org/10.1130/B31838.1; 14 figures; Data Repository item 2018098.

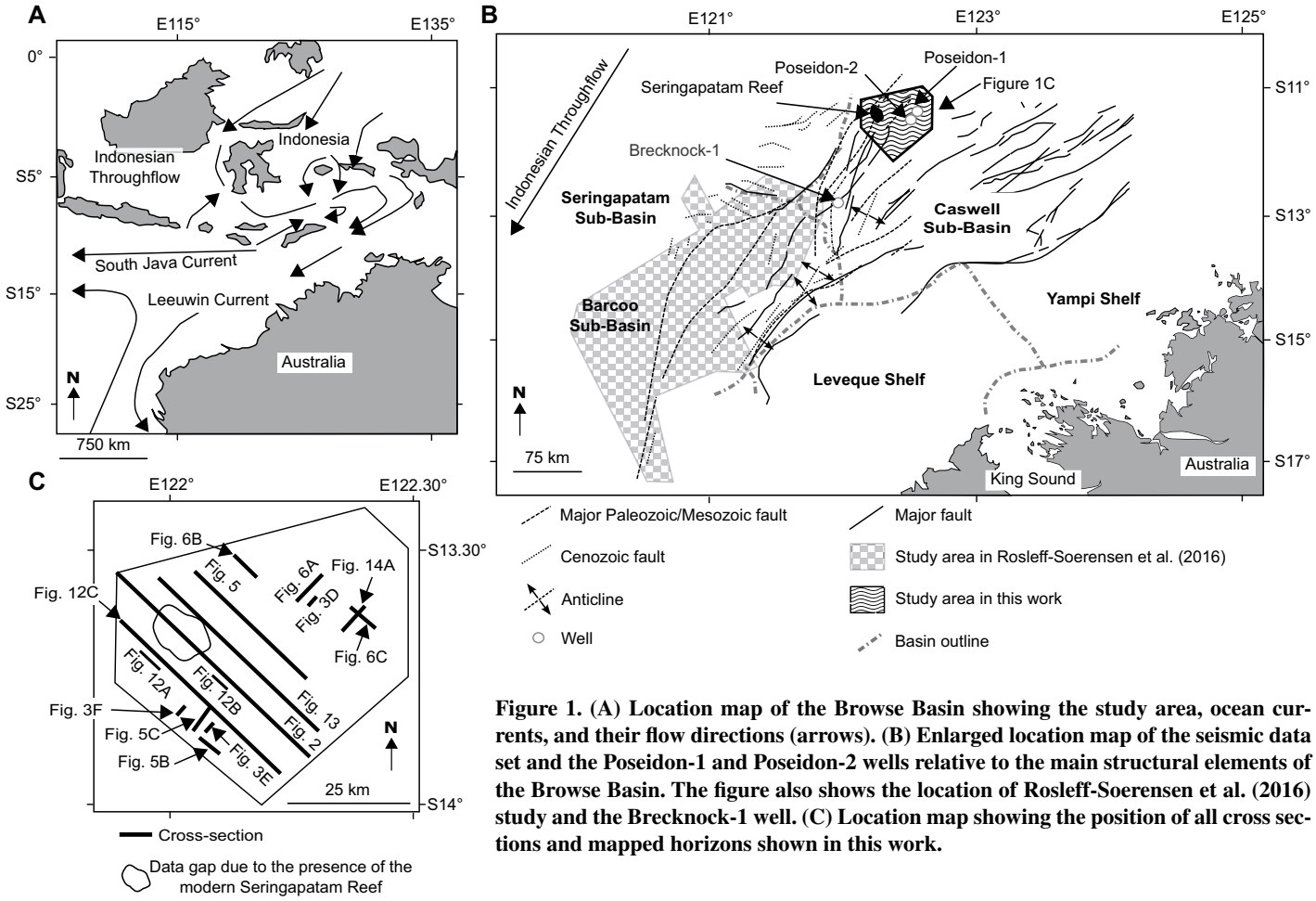

Figure 1. (A) Location map of the Browse Basin showing the study area, ocean currents, and their flow directions (arrows). (B) Enlarged location map of the seismic data set and the Poseidon-1 and Poseidon-2 wells relative to the main structural elements of the Browse Basin. The figure also shows the location of Rosleff-Soerensen et al. (2016) study and the Brecknock-1 well. (C) Location map showing the position of all cross sections and mapped horizons shown in this work.

1997; Gallagher et al., 2009; Kuhnt et al., 2004; Rosleff-Soerensen et al., 2012). The Indonesian Throughflow flooded the North West Shelf with warm, low-salinity water, delivering Pacific and Asian reef species (Collins, 2010; Rosleff-Soerensen et al., 2012). Bathymetric controls on the Indonesian Seaway during Miocene convergence between Australia and the Banda arc (McGowran et al., 1997) strengthened the Indonesian Throughflow (Gallagher et al., 2009; Rosleff-Soerensen et al., 2012) and are thought to have extended carbonate production up to 29°S, along Australia, by the Holocene (Zhu et al., 1993).

Regional Stratigraphy and Associated Petroleum System

The seismic-stratigraphic framework of the Browse Basin is summarized in Figure 2. The Browse Basin petroleum system consists of Lower–Middle Jurassic source rocks, namely, fluvio-deltaic to marine coals and shales deposited during the synrift stage (Fig. 2; Tovaglieri and George, 2014). These Jurassic source rocks reached maturity and started expelling hydrocarbons during the Miocene (Blevin et al., 1998a; Grosjean et al., 2016). The Lower–Middle Jurassic Plover Formation (synrift) forms the major sandstone reservoir in the Browse Basin. Postrift strata include Upper Jurassic organic-rich marine shales (Stephenson and Cadman, 1994; Rosleff-Soerensen et al., 2012; Grosjean et al., 2016), and interbedded Lower Cretaceous shales and carbonates with thin hydrocarbon-bearing turbidites (Stephenson and Cadman, 1994).

Argillaceous carbonates became prevalent in the Browse Basin during the Paleocene (Fig. 2; Apthorpe, 1988). An Eocene–early Oligocene carbonate ramp developed before a stratigraphic break recording uplift and erosion of the inner shelf (Fig. 2; Stephenson and Cadman, 1994; Howarth and Alves, 2016; Belde et al., 2017). Thereafter, a relative sea-level fall resulted in the accumulation of shallow-marine carbonates and the evolution of a late Oligocene–Miocene rimmed platform (Fig. 2; Apthorpe, 1988; Howarth and Alves, 2016; Belde et al., 2017). In summary, the Miocene and Pliocene sections of the Browse Basin represent an aggradational carbonate shelf. The Miocene rimmed platform was drowned in the late Miocene and largely buried by Pliocene hemipelagic sediment (Rosleff-Soerensen et al., 2012; Belde et al., 2017), whereas the modern-day Seringapatam Reef is locally emergent (Fig. 2; ConocoPhillips, 2012).

Faults

The reactivation of Jurassic faults and regional tectonic inversion that occurred after the onset of subduction in the Timor Trough resulted in highly variable deformation styles across the Browse Basin (Harrowfield and Keep, 2005). Small-scale normal faults crosscut late Oligocene–Miocene strata in the eastern part of the study area, forming east-trending lineaments on the sea floor (Howarth and Alves, 2016). While no other faults offset the Miocene sequence, it is noted that sub-seismic-scale fractures and faults may be present and control fluid flow. In addition, late Miocene inversion is documented in the southern Browse Basin (Rosleff-Soerensen et al., 2016).

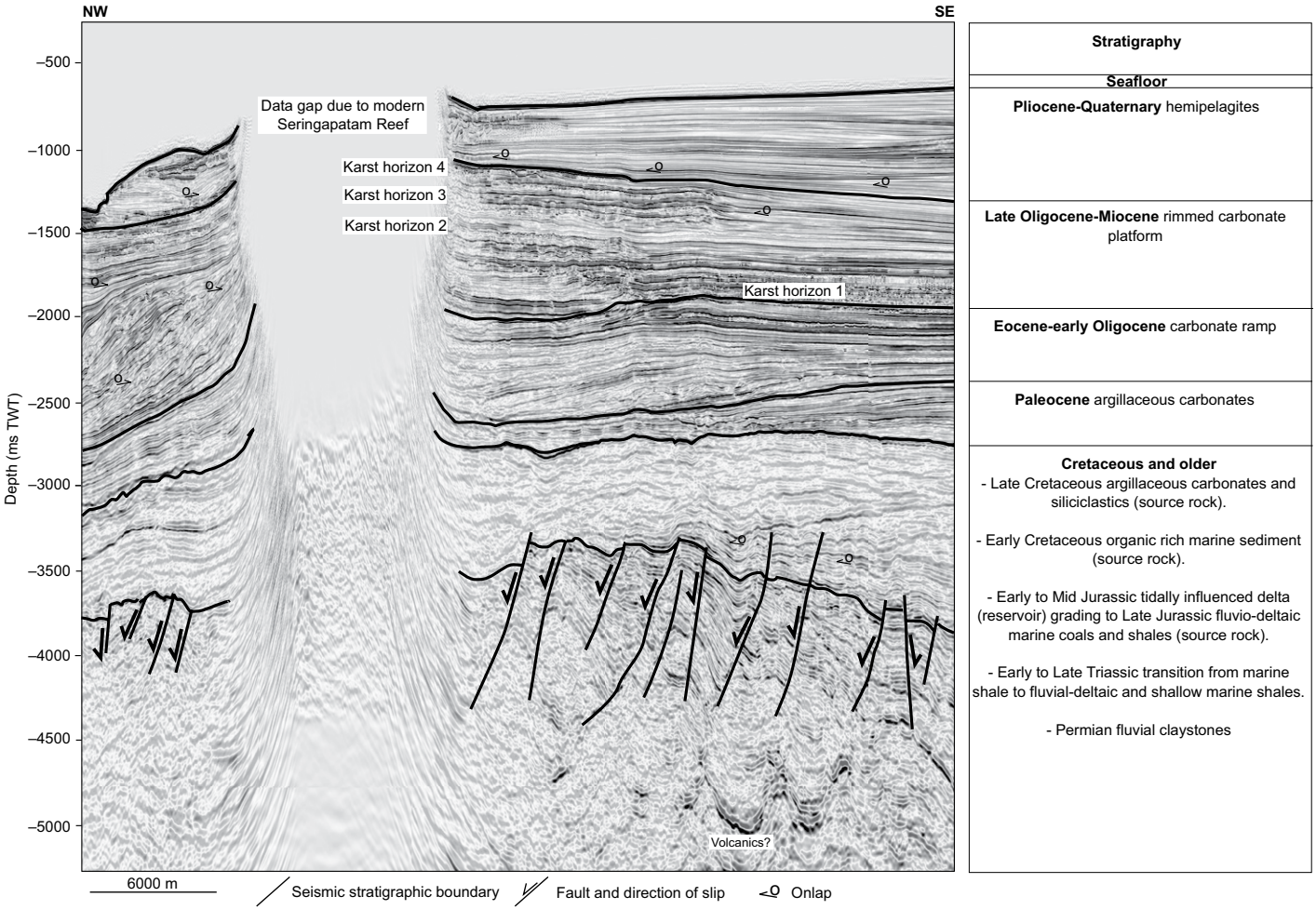

Figure 2. Two-way time (TWT) seismic profile showing the seismic stratigraphy and chronostratigraphy of each unit, as well as their associated depositional environments and elements of the petroleum system (after Australian Geological Survey Organisation North West Shelf Study Group, 1994; Howarth and Alves, 2016) in the study area. The focal point of this study is the late Oligocene–Miocene rimmed carbonate platform, which developed above an Eocene–early Oligocene carbonate ramp. At depth, a passive-margin sequence buries the rift-related topography. A gap in the seismic data (see the western portion of the survey) is due to the presence of the shallow-water Seringapatam Reef, across which seismic data could not be acquired. Associated migration effects are observed at the edge of this data gap.

In parallel with other studies on the North West Shelf, tectonic inversion has been used to suggest faulting as the key control on Cenozoic carbonate growth offshore Northwest Australia (Saqab and Bourget, 2015; Courgeon et al., 2016; Rosleff-Soerensen et al., 2016). However, Howarth and Alves (2016) found no evidence in the study area for direct control by underlying faults on the initiation or distribution of isolated carbonate buildups.

KARSTS

Under the right conditions, the dissolution of carbonate rocks by water can develop extensive porosity (Field, 1999; Wright et al., 2014). As such, karsts and paleokarsts represent key plays within carbonate-hosted reservoirs worldwide, namely, in hydrocarbon fields in China (Han et al., 1998; Liu et al., 2004), Texas (Loucks and Anderson, 1985; Kerans, 1988), Thailand (Heward et al., 2000), Middle East (Harris et al., 1984; Lindsay et al., 2006), and in the "Golden Lane," Gulf of Mexico (Carrasco, 2003). Occurring at multiple scales, karsts are commonly observed along regional unconformities and platform margins due to dissolution of carbonate promoted by groundwater in the meteoric vadose and phreatic zones. An additional process generating karsts is the enhanced mixing of meteoric waters with sea water (mixing corrosion) on platform margins (Wright et al., 2014).

Karsts are regularly identified on seismic data by computing variance maps and time slices. They form negative-relief features with high variance, and are often circular in shape. In some cases, karsts generate a network pattern, as described in Collon-Drouaillet et al. (2012). Such a pattern is often dendritic (or branchwork) on attribute maps.

Howarth and Alves (2016) identified three karst horizons within the Upper Oligocene–Miocene sequence of the Browse Basin. The greatest density of karsts occurring to the southeast, above the inner ramp of the platform, was interpreted to mark prolonged subaerial exposure. Smaller populations of karsts were recorded on the platform margin and northwest edges of isolated carbonate buildups, and these likely represent short-lived exposure events (Howarth and Alves, 2016).

Fluid Flow

Fluids move buoyantly within a sediment body, both laterally and vertically. The migration pathways for fluids are unique to each basin

and are a function of fracture flow, Darcy flow, and diffusion (Kroos and Leythaeuser, 1996). The point where fluid reaches the sea floor, or the surface, is termed a "cold seep" (Judd and Hovland, 2007).

Fluid-flow features are commonly observed on tectonically active continental shelves, settings that are characterized by high sedimentation rates, or they occur near petroleum fields where sediment is overpressured (Osborne and Swarbrick, 1997; Rogers et al., 2006). Key examples include the Gulf of Cádiz (Somoza et al., 2003), offshore Malaysia (Fathiyah Jamaludin et al., 2015), central North West Shelf of Australia (Jones et al., 2006; Rollet et al., 2009; Logan et al., 2010), and offshore Namibia (Moss and Cartwright, 2010). Fluid migration follows the path of greatest permeability, either exploiting differences in porosity and permeability between carbonate facies, or due to the effect(s) of faults and fractures on seal capacity, with or without juxtaposition of permeable strata on either side of a regional seal (Løseth et al., 2009; Frazer et al., 2014; Serié et al., 2016). Similarly, pore-fluid pressure gradients can develop between lithologies with different compressibility characteristics (e.g., carbonates and compressible fine-grained basin sediments), where fluids are laterally forced out of compressible units (Frazer et al., 2014).

The identification and evaluation of fluid-flow pathways are key steps in reducing hydrocarbon exploration uncertainty (Cartwright, 2007; Moss and Cartwright, 2010). In the Browse Basin, O'Brien et al. (2005) documented seeping dry gas and oil on the sea floor of the Yampi Shelf, which provides evidence for hydrocarbon flow to the southeast of the study area.

Fluid Flow and Isolated Carbonate Buildups

Based on Hovland (1990), seep-reef relationships include: (1) carbonate buildups associated with salt diapirs, where a carbonate buildup develops above a salt diapir as the result of enhanced fluid flow around the latter structure, (2) mud diapir–associated carbonate buildups, where the upwelling of warm mud and methane provides a food source and a topographic high to attract reef-building organisms (Hovland, 1990), and (3) methane-derived carbonates, formed where colonies of archaea and bacteria in the sediment column use seeping methane as a food source (Roberts et al., 1993; Judd and Hovland, 2007). In this latter case, carbonate precipitation occurs at the seep and follows specific chemical reactions (Peckmann et al., 2001; Hovland et al., 2012):

$$CH_4 + SO_4^{2-} \rightarrow HCO_3^- + HS^- + H_2O. \quad (1)$$

$$Ca^{2+} + 2HCO_3^{2-} \rightarrow CaCO_3 + H_2O + CO_2. \quad (2)$$

Methanogenic carbonates either form seepage-associated carbonates or chemoherm carbonates. The latter form a buildup of precipitated chemical carbonates with the calcareous skeletal debris of chemosynthetic fauna producing a structure up to 90 m high (Teichert et al., 2005) under sustained seepage of methane-rich fluids into bottom waters (Han et al., 2008). Seepage-associated carbonates occur at the sea floor or subsurface as carbonate slabs, concretions, crusts, and tubes, interpreted to represent slower fluid-flow regimes (Han et al., 2008).

Carbonates formed by anaerobic oxidation of methane usually occur in deep, cold, and anoxic waters (Michaelis et al., 2002; Aloisi et al., 2002; Wild et al., 2015). Few have been documented in shallow tropical waters (e.g., Wild et al., 2015), because oxic conditions cause aerobic oxidation of CH_4 and the widespread production of CO_2. However, this does not mean methanogenic carbonates cannot occur in oxic conditions, as methane anoxia can create localized anoxic environments near fluid pathways (Wild et al., 2015).

DATA AND METHODS

This work uses a 3-D seismic volume covering 2851 km^2 of the Browse Basin, on the shelf margin (Fig. 1). The seismic survey was acquired in a direction parallel to the northwest-striking continental shelf and is not aligned with the long axis of fluid-venting structures, or with any karst networks. Therefore, no spatial aliasing occurred when imaging shallow features (Ho et al., 2012). The data set follows the Society of Exploration Geophysicists (SEG) European polarity convention, i.e., an increase in acoustic impedance equals a red reflection of negative amplitude (Rosleff-Soerensen et al., 2016).

The interpreted data set includes two exploration wells, Poseidon-1 and Poseidon-2 (Fig. 1). Poseidon-1 is a wildcat and recorded the first gas discovery in the Browse Basin (Poseidon field). It provided gamma-ray data, including the rate of penetration and resistivity data from 4000 to 6000 meters below the sea floor (mbsf). The Poseidon-2 well was drilled to assess the presence and nature of the gas in the Plover Formation. It provided lithological data below 2430 mbsf (Howarth and Alves, 2016). Both wells cross the Upper Oligocene–Miocene sequence, but neither sampled an isolated carbonate buildup directly. As a result, isotope data used in this work was acquired at the Brecknock-1 well (Fig. 1), which sampled the same carbonate sequence ~75 km to the southwest of the study area (Rosleff-Soerensen et al., 2016).

Faults were mapped manually every 10 inlines and crosslines. Ninety-one (91) pinnacle features were also mapped in areas where seismic reflections exhibited a sharp, conical geometry (Fig. 3). They are distinct from velocity pull-ups, which are the result of sharp subsurface velocity contrasts because they comprise localized features within larger isolated carbonate buildups and overlie flat seismic reflections (Fig. 3). Horizon mapping for every inline and crossline was undertaken to image the morphology of pinnacle features (Fig. 3).

The depths, volumes, heights, and slope angles of pinnacle features were measured in milliseconds two-way time (TWT) using Petrel®, and histograms were generated for height and volume. A general velocity of 3.0 km/s was used when converting TWT depth to true depth based on data from Rosleff-Soerensen et al. (2016). The volume of individual pinnacles was calculated using the equation:

$$V = \pi \times r^2 \times (h/3). \quad (3)$$

This equation represents the volume of a cone, with V being the volume of pinnacle features, π representing pi (3.14159), r being the radius of the pinnacles, and h being their height. Slope angles were calculated taking into account a P-wave (V_p) velocity of 3.0 km/s to convert TWT depth to true depth in meters, using the equation:

$$\text{Angle } x = \tan^{-1} (\text{opposite/adjacent}). \quad (4)$$

The presence of fluid in subsurface strata was interpreted through the identification of seismic anomalies. These included bright spots, flat spots, phase reversal associated with accumulated hydrocarbons, and hydrocarbon-related diagenetic zones (O'Brien and Woods, 1995; Logan et al., 2010). Vertical dim zones and vertical bright zones were also mapped, because they result from the scattering, attenuation, and decrease in the velocity of compressional waves (P waves) as they pass through gas-charged zones (Løseth et al., 2009; Fathiyah Jamaludin et al., 2015).

Mud volcanoes and pockmarks are surface expressions of fluid flow (Løseth et al., 2009; Moss and Cartwright, 2010), and were interpreted in the study area. Mud volcanoes exhibit circular to subcircular conical geometries, with slope angles up to 30° and a flat top that generates a high-amplitude reflection (Somoza et al., 2003). Pockmarks are crater-shaped erosional depressions formed in soft fine-grained seafloor sediment (Hovland and Judd, 1988).

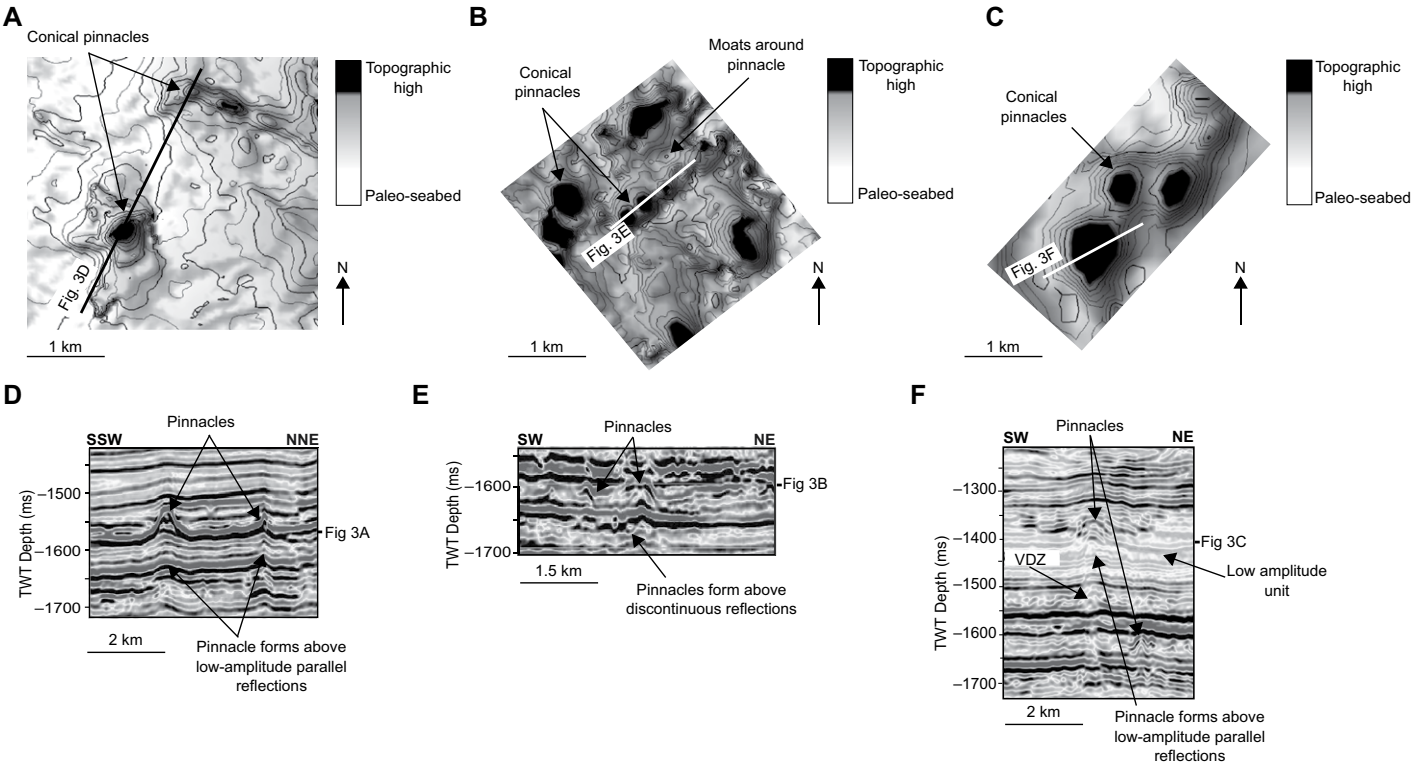

Figure 3. (A–C) Two-way time (TWT) structural maps of key seismic horizons and (D–F) corresponding cross-sections highlighting the seismic and morphological characters of pinnacle features in the study area. Pinnacle features produce cone-shaped topographic highs on the sea floor. In cross section, pinnacles often have a high-amplitude reflection on top, while their interior is of lower amplitude with occasionally evidence for layering. VDZ—vertical dim zone.

Velocity pull-ups and push-downs are caused by contrasts in the seismic velocity of distinct lithologies, e.g., carbonate and shales. To accurately interpret velocity pull-ups as fluid-flow features, the areas showing seismic anomalies were compared to known examples of fluid flow (Jones et al., 2006; Rollet et al., 2009; Logan et al., 2010; Fathiyah Jamaludin et al., 2015).

The variance attribute was applied to the seismic volume to highlight discontinuities in, or between, seismic reflections that generated high variance (Howarth and Alves, 2016). As such, it was useful for imaging subtle stratigraphic features that generated 3-D offsets, such as karsts, faults, and fluid pipes (Omosanya and Alves, 2013; Marfurt and Alves, 2015).

RESULTS

Faults

Structural mapping and variance data revealed three fault families (Fig. 4, supplementary Figs. DR1–DR3).[1] The first family consists of northeast-striking extensional faults that are parallel to the shelf margin and that dip northwest and southeast (Fig. 4 and DR1 [see footnote 1]). These faults are laterally continuous features that cause large displacements within pre-Cenozoic strata and generate significant fault block topography (Fig. 2). Faults tip-out within overlying Cretaceous strata, but they were not observed to offset Paleocene units.

The second family of faults also consists of northeast-striking extensional structures parallel to the shelf margin. They are confined to the break in slope of the Eocene–early Oligocene ramp (Figs. 2, 4, and DR2 [see footnote 1]). None of the faults observed in this family was related to the position of isolated carbonate buildups or appeared to influence isolated carbonate buildup morphology (Fig. 4).

The third fault family consists of east-striking extensional faults that are near-perpendicular to the shelf margin. These faults offset Pliocene to Eocene strata and show relatively small throws. No growth structures were observed within Upper Oligocene–Miocene strata, and faults in this family were confined to the eastern part of the study area (Figs. 2, 4, and DR3 [see footnote 1]).

Karsts

Within the Lower Oligocene–Miocene sequence, four (4) horizons are characterized by chaotic to discontinuous seismic reflections (Fig. 5). Lateral interruptions in seismic reflections generate high-variance, negative-relief features that are greater than 60 m in diameter. Horizon 1 occurs from –1750 ms to –1900 ms across the top Eocene boundary into Lower Oligocene–Miocene strata. It is characterized by pervasive circular topographic depressions (Figs. 5A and 5B). In a number of examples, this negative relief is linear and shows a branchwork pattern across the ramp interior. Seismic reflections become continuous along this horizon. To the southwest, they develop sigmoid to sigmoid-oblique geometries, which reveal successive phases of progradation toward the southeast (Fig. 5).

Horizon 2 also shows discontinuous seismic reflections associated with high-variance negative topography clustering within the isolated carbonate buildups (Fig. 5). Discrete, high-variance, circular depressions commonly reveal a branchwork pattern, with individual depressions showing a minimum diameter of 60 m (Figs. 5A and 5B).

[1]GSA Data Repository item 2018098, Figures DR1–DR3, is available at http://www.geosociety.org/datarepository/2018 or by request to editing@geosociety.org.

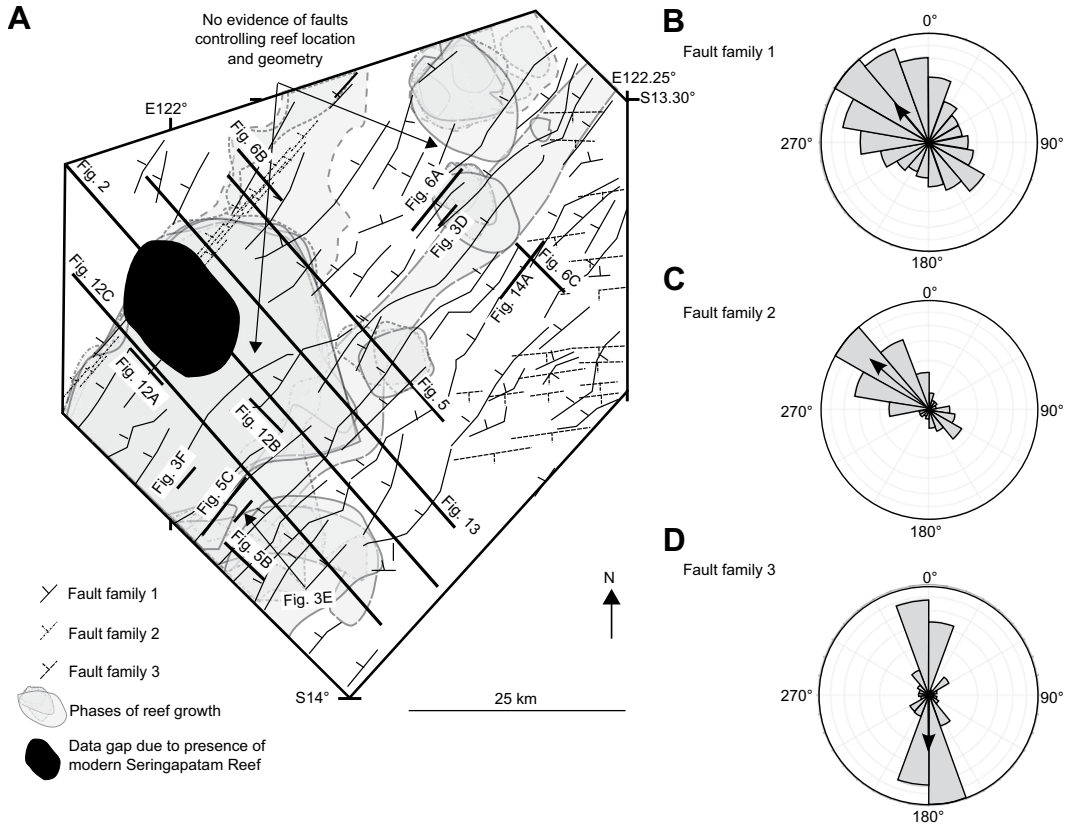

Figure 4. (A) Map showing the three fault families identified in the study area and their positions relative to late Oligocene–Miocene isolated carbonate buildups (please see Supplementary Fig. DR1–DR3 [see text footnote 1]). (B–D) Rose diagrams showing structural data (dip direction) for each fault family. Fault family 1 strikes northeast and chiefly includes northwest-dipping extensional faults formed during Mesozoic rifting. Their fault block topography is buried by the passive-margin sequence. Fault family 2 strikes northeast and includes northwest-dipping extensional faults, which were confined to the margin of the underlying Eocene–early Oligocene ramp. These faults mark the edge of the basin margin, which controlled the northwest extent of Miocene progradation. Fault family 3 strikes roughly to the east and includes south-dipping extensional faults that are confined to the platform interior. These faults offset Miocene strata, but no growth patterns were observed, suggesting they postdated the Miocene and were associated with plate collision and subduction at the Timor Trough. The relative positions of isolated carbonate buildups show no relationship to underlying faults, suggesting these latter played no role in controlling the geometries and locations of isolated carbonate buildups.

Horizon 3 documents the same character to horizons 1 and 2 (Fig. 5). Growth patterns show build-out and build-down geometries, while isolated carbonate buildups are characterized by discontinuous seismic reflections in the northern part of the study area.

The fourth horizon (horizon 4) occurs between –1150 ms and –1200 ms at the top of the Upper Oligocene–Miocene sequence (Fig. 5). Similar to horizons 2 and 3, these circular features show high variance values and diameters greater than 60 m (Fig. 5A).

Pinnacle Features

Within the Upper Oligocene–Miocene sequence, 91 discrete seismic reflections exhibit circular to subcircular, conical geometries (Fig. 3). We refer to these features as pinnacles or pinnacle features.

Pinnacles are high-amplitude, continuous seismic reflections that are onlapped by low-amplitude strata (Figs. 3 and 6). Pinnacles typically have slope angles reaching a maximum of 8°. Their height ranges from 31 m to 174 m, with an average of 77 m and a mode of 66 m (Fig. 7A). The histogram in Figure 7B shows a normal distribution for pinnacle heights with a positive skew. Interpreted pinnacles range in volume from 33 km^3 to 11,105 km^3, with an average of 2424 km^3 and a mode of 780 km^3 (Fig. 7A). The histogram in Figure 7C reveals a strong positive skew, with a sharp decline in the frequency of pinnacle exceeding 3000 km^3 in volume.

Internally, pinnacle features show relatively low amplitudes, but some reveal evidence of layering. However, the interpretation of their internal character becomes increasingly difficult as pinnacle reflection size decreases, especially where pinnacle diameters are at the lower limit of seismic resolution. When separated according to depth, pinnacle features show a linear northeast trend during the early stages of isolated carbonate buildup growth (Fig. 8). Importantly, this linear trend follows the break in slope of the underlying carbonate ramp.

Subsequent pinnacle features appear basinward to the northwest and show increasingly clustered distributions within isolated carbonate buildup interiors on the basin margin, and in the northeast of the study area (Figs. 8, 9, 10, and 11). Their positions mirror isolated carbonate buildups and the locations of karst horizons (Figs. 5, 8, 9, and 10). Pinnacle features are scarce within parallel, low-amplitude reflections that onlap isolated carbonate buildups, notably within a northwest-trending corridor in the center of the study area, as well as in the southeast (Figs. 8, 9, 10, and 11).

Pinnacles are commonly onlapped by seismic reflections over which larger isolated carbonate buildups have developed (Fig. 6). Seismic reflections in the larger isolated carbonate buildups exhibit sigmoidal to sigmoidal-oblique geometries (Fig. 6). However, significant variations in their geometry were observed when individual isolated carbonate buildups were compared.

Fluid Flow and Associated Seismic Anomalies

Vertical to subvertical zones of discontinuous and suppressed seismic reflections (vertical dim zones) were observed throughout the 3-D seismic volume (Figs. 8, 9, 10, and 11). The spatial distribution of vertical dim zones beneath the top ramp horizon appears random in the southeast of the study area, but shows an increasingly

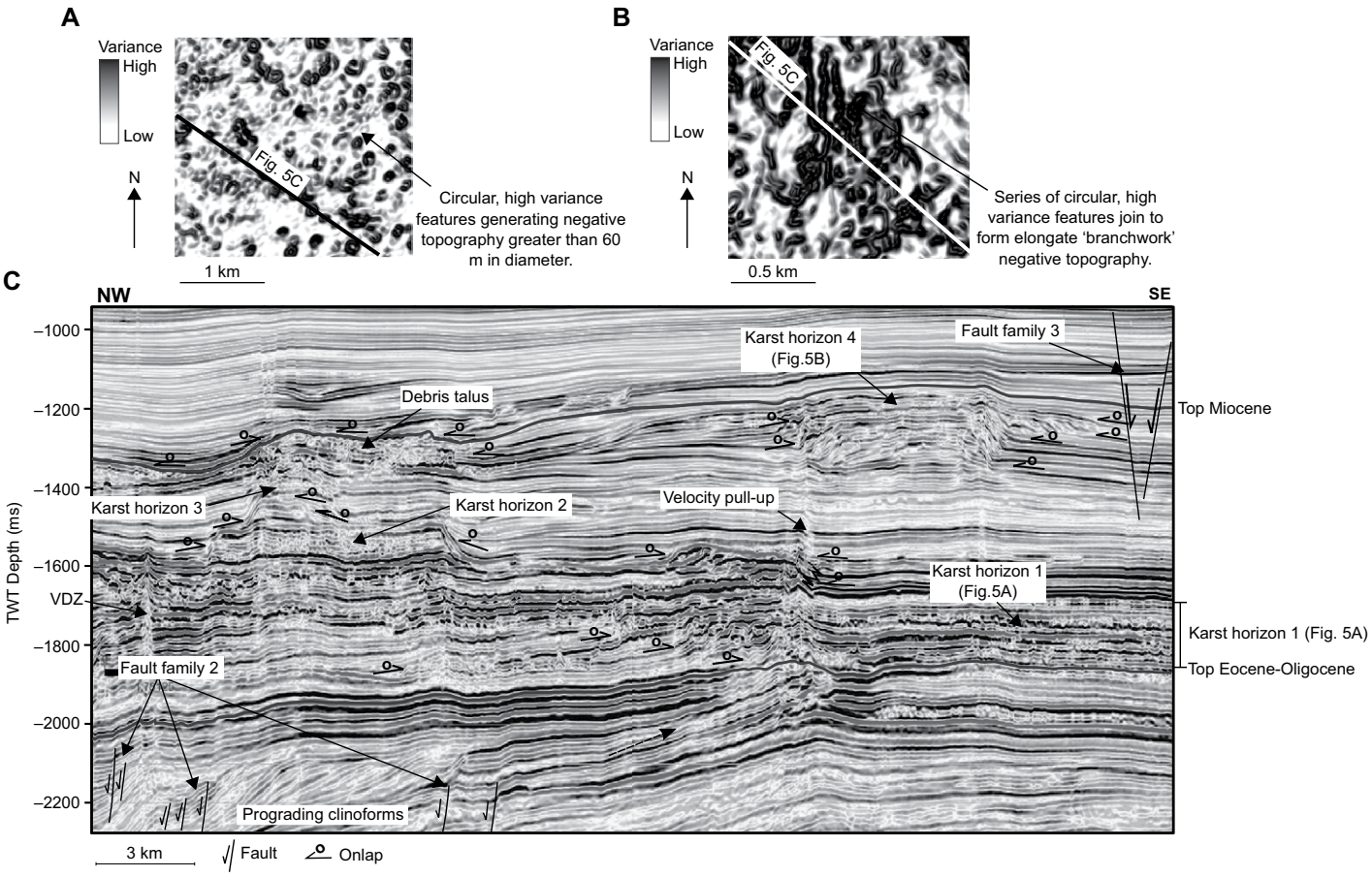

Figure 5. (A) Variance slice through karst horizon 1 at z = –1150 ms TWT, showing pervasive circular features with high variance interpreted as karsts. Individual karsts are greater than 60 m in diameter. (B) Variance slice through karst horizon 4 at z = –1750 ms TWT, showing pervasive circular features, with high variance and diameters greater than 60 m. Some of these interpreted karsts form networks and elongate geometries typical of branchwork patterns (Collon-Drouaillet et al., 2012). (C) Interpreted two-way time (TWT) seismic profile showing the location of the four karst horizons, as well as fault families 2 and 3. Fault families 2 and 3 comprise extensional faults. Neither family generated enough topography to influence the positions or geometries of isolated carbonate buildups. Karsts in horizon 1 are the largest and most extensive of the four mapped horizons, while karsts in horizons 2, 3, and 4 are predominantly confined to the interiors of isolated carbonate buildups.

linear distribution to the northwest (Fig. 8). This linear distribution reveals a northeast trend to vertical dim zones that mirrors the strike of pre-Miocene fault families (Fig. 8). Furthermore, this northeast trend matches the strike of progradational clinoforms within the Eocene–early Oligocene ramp (Fig. 8).

The spatial distribution of vertical dim zones becomes increasingly clustered moving upwards through the Upper Oligocene–Miocene sequence, focusing within isolated carbonate buildup interiors along the basin margin (Figs. 8, 9, 10, and 11). Throughout the Upper Oligocene–Miocene sequence, the distribution of vertical dim zones is associated with isolated carbonate buildups (Fig. 8). This is particularly shown in Figure 9, where low-variance and low-amplitude strata bury part of the large shelf margin. In contrast, vertical dim zones and pinnacles are no longer observed within the areas buried by low-variance seismic facies in the platform interior, or along a northwest-trending transect in the middle of the study area (Figs. 8, 9, 10, and 11). Instead, vertical dim zones and pinnacles occur within the high-variance isolated carbonate buildups (Figs. 8, 9, 10, and 11).

The majority of vertical dim zones terminate within Pliocene strata (Fig. 11). Smaller numbers of localized amplitude anomalies, pockmarks, and mud volcanoes are observed in Pliocene–Quaternary strata and on the sea floor, particularly around the Seringapatam Reef (Fig. 12). In addition to vertical dim zones, seismic washouts are observed within steep clinoforms on the northwest margins of isolated carbonate buildups and their interior (Fig. 12). Their presence is highlighted by a notable increase in the amplitude of seismic reflections on the southeast margins of isolated carbonate buildups, which typically show a more continuous nature (Fig. 12). In these areas, bright spots (Fig. 12) are often laterally continuous and range typically from 100 m to ~1 km in length. In some cases, bright spots are vertically stacked around vertical dim zones (Fig. 12). Bright spots can also be seen in horizons characterized by discontinuous seismic reflections, as well as vertical dim zones (Fig. 12).

Figure 12 shows conical topographic highs on the modern sea floor that are characteristic of mud volcanoes and steep-sided depressions suggestive of pockmarks. These features are observed above vertical dim zones, bright spots, and areas of seismic washout, particularly around the Seringapatam Reef. In parallel, velocity pull-ups are observed beneath the margins of the largest isolated carbonate buildups, which

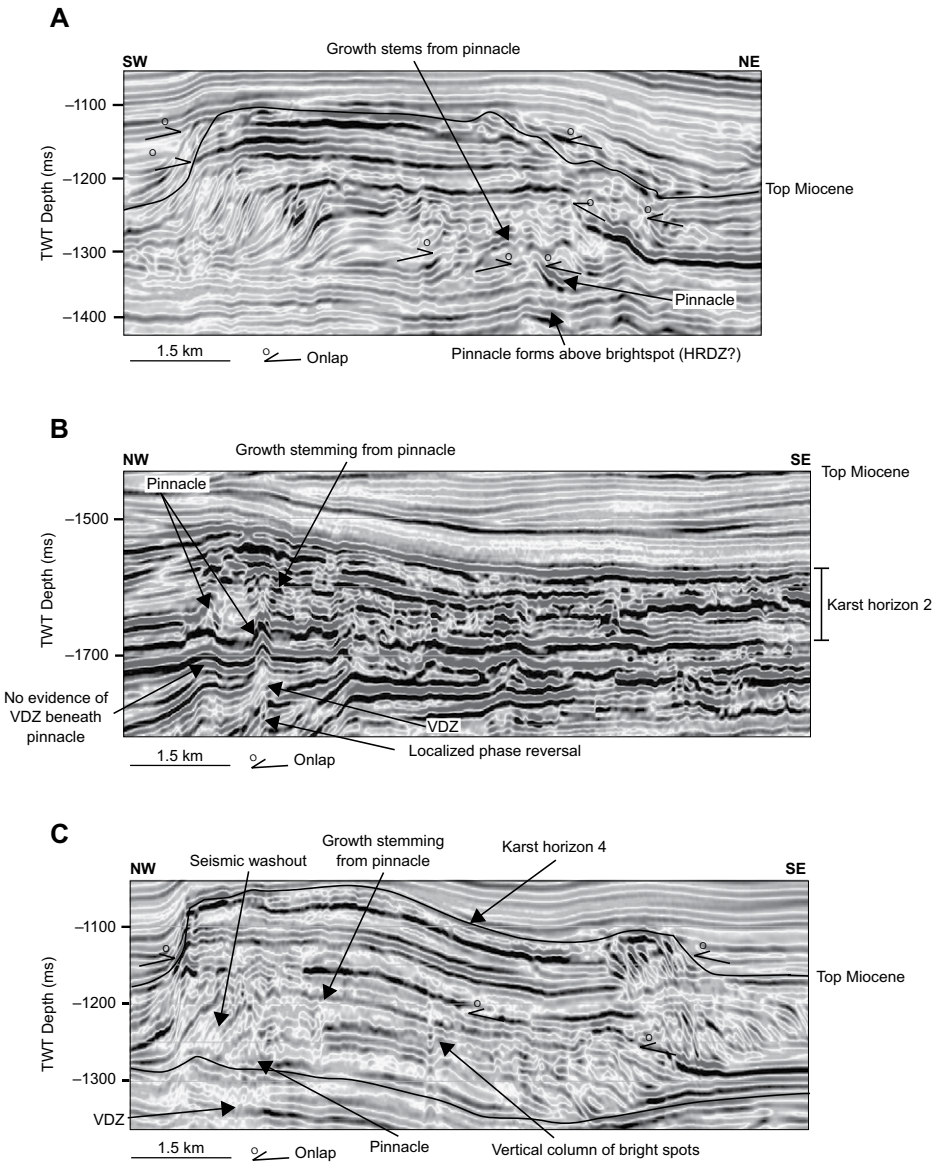

Figure 6. (A–C) Two-way time (TWT) seismic profiles showing high-amplitude seismic reflections in isolated carbonate buildups, stemming from the pinnacles. Initially, high-amplitude reflections onlapped the pinnacles and eventually buried them. This suggests that the topography generated by the pinnacles provided an area for preferential growth of isolated carbonate buildups. The geometries exhibited by the overlying reflections are highly variable and indicate that isolated carbonate buildup growth was subject to local environmental and oceanographic conditions. The seismic profile in C also shows pinnacles that are not underlain by vertical dim zones (VDZs). Instead, seismic profiles may exhibit localized bright spots (A), while others show no evidence of seismic anomalies (B). These latter observations suggest that not all pinnacles are formed by the same geological process. HRDZ—hydrocarbon-related diagenetic zone.

are onlapped by lower-amplitude horizontal reflections (Fig. 6). Underlying seismic reflections dip upward and mirror the geometry of the overlying isolated carbonate buildup. In some cases, a discontinuous character comparable to vertical dim zones is observed beneath the margins of isolated carbonate buildups (Fig. 6C).

Relationship between Pinnacle Features and Seismic Anomalies

A causal relationship is thus recorded between pinnacle features and vertical dim zones (Figs. 3 and 8). During the initial stages of isolated carbonate buildup growth, pinnacle features are observed directly above the areas with the highest concentration of seismic anomalies (Figs. 8 and 9). Thereafter, the spatial distribution of vertical dim zones and other seismic anomalies correlates with the position of the Miocene isolated carbonate buildups (Fig. 10).

Pinnacles are not commonly observed within the thick units of low-amplitude, laterally continuous onlapping reflections against which vertical dim zones often terminate (Figs. 3 and 9). In addition, not all pinnacles sit above seismic anomalies. Some sit beneath the margins of isolated carbonate buildups (Fig. 9), while others sit above strata lacking seismic anomalies (Fig. 6B).

DISCUSSION

Where Are the Main Sources for Fluids in the Browse Basin Located?

Our results document a number of seismic anomalies that resemble fluid-flow features recorded elsewhere on the North West Shelf (Fig. 12; O'Brien and Woods, 1995; Jones et al., 2006; Rollet et al., 2009, Logan et al., 2010). The distribution of fluid-flow features in specific areas of the late Oligocene–Miocene platform, and their association with pre-Miocene faults (Fig. 12) could be attributed to a biogenic origin. However, when analyzed in combination with the Browse Basin petroleum system, the distribution of fluid-flow features in the study area is suggestive of deeper fluid plumbing (Serié et al., 2016). Hydrocarbon leakage from deep reservoirs is a common occurrence in the Timor Sea (Gartrell et al., 2003), Malay Basin (Ghosh et al., 2010), Australian Basin (Logan et al., 2010), and other hydrocarbon-producing areas worldwide (Schroot et al., 2005; Fathiyah Jamaludin et al., 2015). In the Browse Basin, hydrocarbon migration is believed to have started as early as the latest Cretaceous (Blevin et al., 1998b) and continued through the Neogene (Grosjean et al., 2016). In parallel, modeling results show that the westerly flexure of the shelf favored hydrocarbon migration toward the basin margins where the late Oligocene–Miocene platform was developing (Blevin et al., 1998a). As Cretaceous shales, comprising the primary seal for a number of plays in the Browse Basin, exhibit variable thickness across the basin (Blevin et al., 1998a), doubts can be raised about its effectiveness as a regional seal interval. We suggest that fluid was likely breaching this seal and reaching successive paleo-seafloors up to, and throughout, the late Oligocene and Miocene.

Blevin et al. (1998a) recognized a number of structural and stratigraphic traps in the

A

	Height (m)	Volume (km^3)
Mean	77.6	2424.2
Mode	66.3	780
Max	374.6	11105
Min	31.5	33

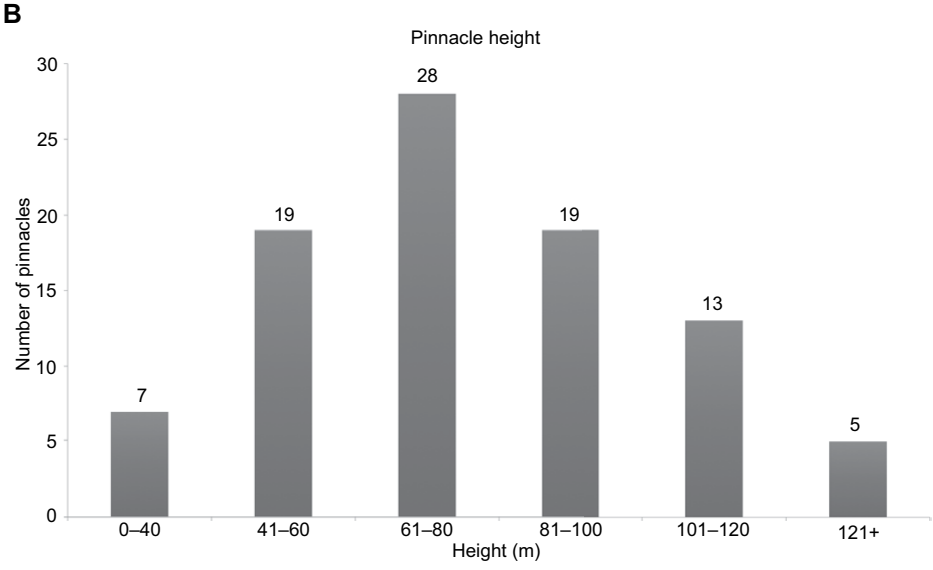

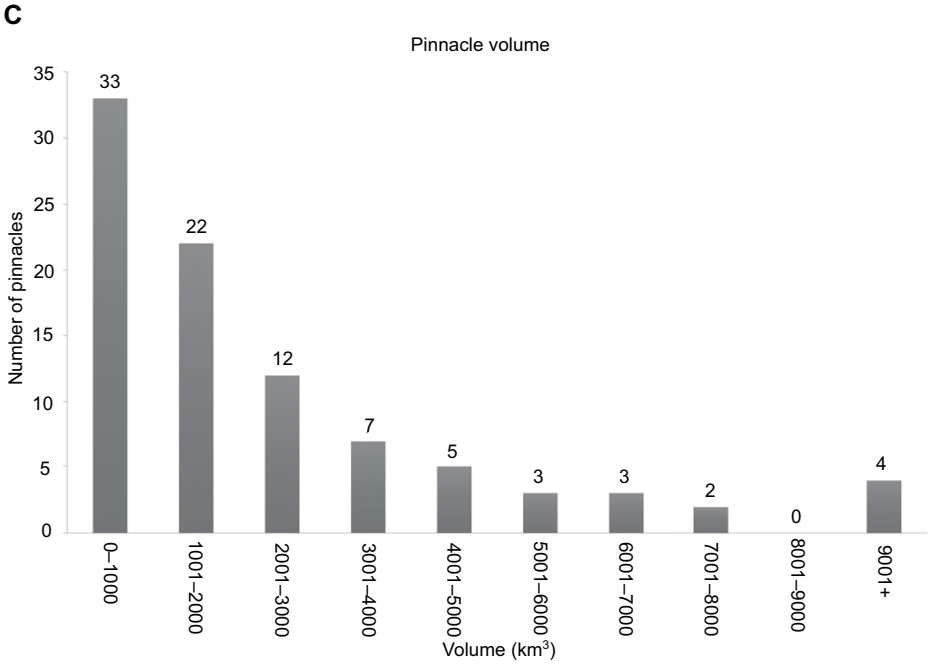

Figure 7. (A) Summary of the mean, mode, and ranges of pinnacle volumes and heights. (B) Histogram showing pinnacle height. Pinnacle heights show normal distribution with a positive skew. Height ranges from 31.5 to 174.6 m, with a mean height of 77.6 m and mode of 66.3 m. The height of pinnacle features generated enough topography to trigger preferential isolated carbonate buildup growth on the Browse Basin shelf. (C) Histogram showing pinnacle volumes. Pinnacle volumes range from 33 to 11,105 km^3, with a mean of 2424.2 km^3 and a mode of 780 km^3. The histogram shows a strong positive skew with a sharp decline in the frequency of pinnacle features with volumes above 3000 km^3.

Browse Basin. Our results show a correlation between the position of vertical dim zones and vertical bright zones and the deeper extensional faults (fault family 1), suggesting that these faults acted as migration pathways for fluid (Figs. 3 and 8). However, fault family 1 does not offset the Eocene–early Oligocene ramp (Fig. 2). As such, their control on fluid flow is expected to diminish away from their upper tips. Faults in extensional fault family 2, within the prograding clinoforms of the Eocene–early Oligocene ramp (Figs. 4 and 13A), do not extend into the Upper Oligocene–Miocene sequence and relate to syndepositional deformation (Rankey, 2017). Fluid-flow distribution suggests this fault family likely created a preferred migration pathway through the Eocene–early Oligocene ramp (Fig. 8).

Comparisons between the distribution of fluid-flow features and depositional facies models for carbonate ramps, as described by Wilson (1975), indicate that fluid migration follows higher-permeability grain-rich facies belts (e.g., boundstones, bafflestones, and grainstones) on the wave-agitated inner ramp (Fig. 13; Ahr, 1973; Read, 1985). It must be noted, however, the striking difficulty in ascertaining the permeability of ramp facies from seismic data alone. The termination of fluid flow features against onlapping, low-amplitude seismic reflections northwest and southeast of the initial isolated carbonate buildup growth sites is interpreted to highlight the seal potential of muddier, finer-grained, lower-permeability facies in outer-ramp and lagoonal areas (Figs. 8, 9, 10 and 11; Ahr, 1973; Read, 1985). When considered in combination with the northwest dip of the Eocene–early Oligocene ramp (Figs. 5C and 13A), this potentially sealing facies facilitates updip migration along bedding planes toward the break in slope, upon which isolated carbonate buildup growth was initiated (Figs. 5C, 8, and 13A).

Based on the observed correlation between fluid-flow features and karstified intervals (Figs. 8, 9, 10, and 11), we suggest that karstification influenced fluid flow by generating secondary permeability and porosity similarly to oil and gas fields in China (Han et al., 1998; Liu et al., 2004), Texas (Loucks and Anderson, 1985; Kerans, 1988), Thailand (Heward et al., 2000), and other carbonate platforms worldwide (Loucks, 1999; Fournillon et al., 2012). We cannot determine permeability and porosity from seismic data alone, as karstification and diagenetic processes associated with the emergence of isolated carbonate buildups are highly variable.

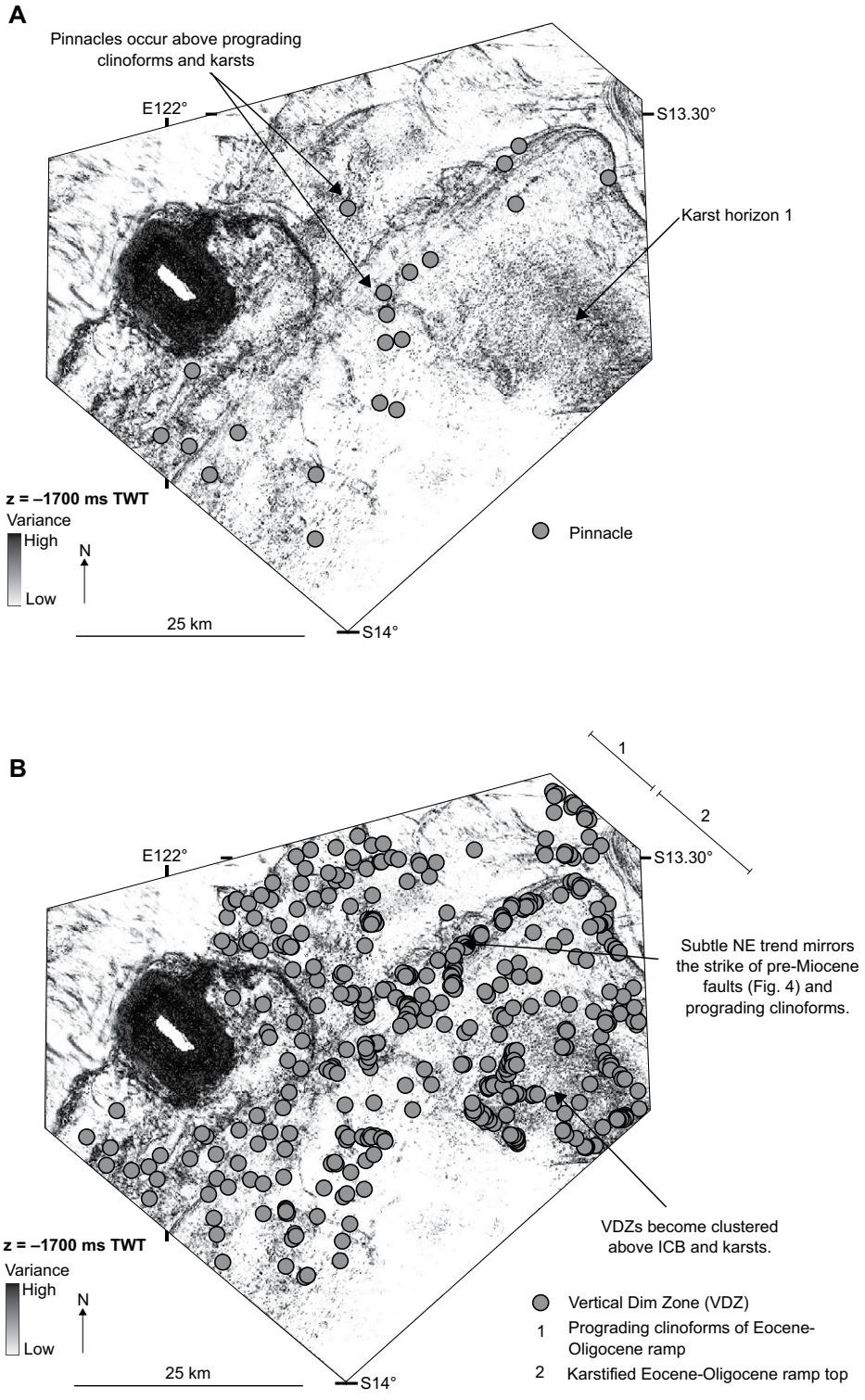

Figure 8. (A–B) Pair of variance slices taken at –1700 ms two-way time (TWT). The variance slices show the position of pinnacles (A) and corresponding vertical dim zones (VDZs; B). The first pinnacles occur above the break in slope and above the karstified interior of the Eocene–early Oligocene carbonate ramp (A). Vertical dim zones show an initial random distribution above prograding clinoforms of the Eocene–early Oligocene carbonate ramp and karstified areas of the ramp interior (B). Subtle NE-trending bands of the vertical dim zones mirror the positions of deeper pre-Miocene faults (Fig. 4), suggesting these areas were favorable for fluid flow. ICB—isolated carbonate buildup.

What Do Pinnacle Features Observed at the Base of Isolated Carbonate Buildups Reflect in Terms of Geological Processes?

In the Browse Basin, the spatial relationship between fluid-flow and pinnacle features indicates that pinnacles are a surface expression of paleo–fluid flow (Figs. 6 and 8; Hovland and Judd, 1988; Milkov, 2000). The conical geometries of pinnacle features match the diagnostic criteria for mud volcanoes as described in Brown (1990) and Kopf (2002); see Figure 3. When compared to the classification scheme of Kalinko (1964), which identified three classes of mud volcano based on the character of their activity with respect to morphological expression (Dimitrov, 2002), the interpreted pinnacle features are suggestive of class 1, Lokbatan-type mud volcanoes. Formed by periodic explosive activity, due to the buildup of pore fluid pressure beneath a blockage in the feeder channel, they extrude low-viscosity mud breccia to form a steep conical-shaped mud volcano (Fig. 14B; Kalinko, 1964; Dimitrov, 2002).

The sizes and slope angles of pinnacle features in the Browse Basin are consistent with mud volcanoes mapped in southwest Taiwan (Chen et al., 2014) and in the Gulf of Cádiz, where single, circular mud volcanoes have bathymetric relief of 80–100 m and slope angles of 6° to 8° (Somoza et al., 2003). Their internal seismic character (Fig. 3) reveals a strong top reflection surface, also characteristic of mud volcanoes in the Gulf of Cádiz (Somoza et al., 2003), where a sharp lithological change occurs between the mud volcano and overlying carbonate sediments (see also Barber et al., 1986; Pickering et al., 1988; Orange, 1990). However, mud volcanoes are not commonly documented in Miocene strata of the North West Shelf (Jones et al., 2006; Logan et al., 2010), probably due to strong ocean currents and wave activity not allowing the formation of stable mounds of the heights we document (Logan et al., 2010; Bachtel et al., 2011). Nevertheless, we documented mud volcanoes on the modern sea floor with heights and slope angles that are comparable to pinnacle features in the Upper Oligocene–Miocene sequence (Fig. 12A). Considering that the present-day North West Shelf is a high-energy, shallow-water environment that experiences macrotides, seasonal cyclonic storms, and long-period swells (James et al., 2004), the presence of pinnacles on the modern sea floor suggests that structures associated with seepage (e.g., pockmarks, mud volcanoes) were not quickly destroyed by currents and waves in the late Oligocene–Miocene Browse Basin (Logan et al., 2010). Instead, the pinnacle features interpreted at depth survived long enough to be colonized by reef-building organisms.

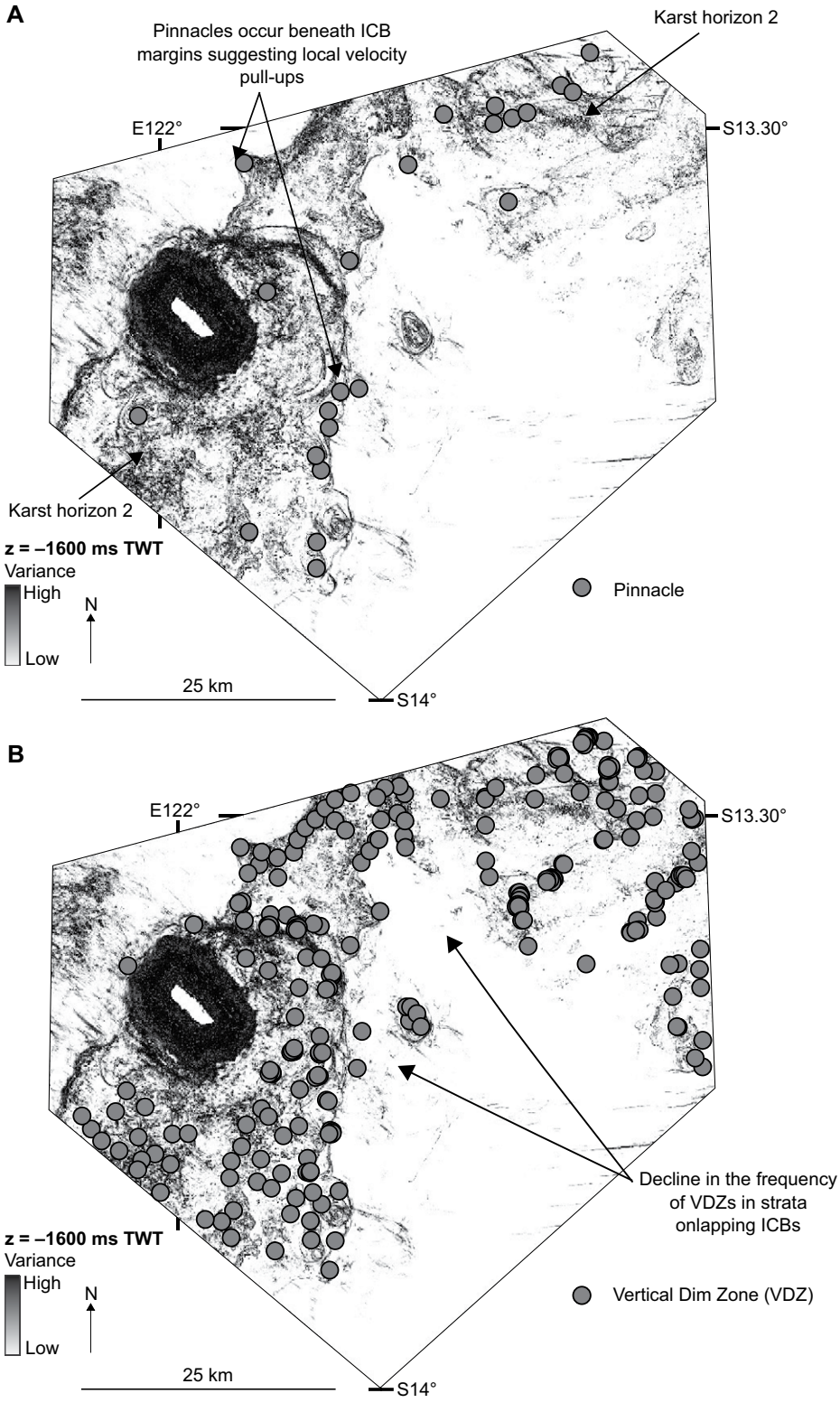

Figure 9. (A–B) Pair of variance slices taken at –1600 ms two-way time (TWT). The variance slices show the position of pinnacles (A) and corresponding vertical dim zones (VDZs; B). *As isolated carbonate buildup (ICB) growth continued, the carbonate system moved to the basin margin and formed a barrier reef. Pinnacles are observed within these isolated carbonate buildups. Several pinnacles occur beneath the margins of the isolated carbonate buildups and likely reflect velocity pull-ups. Vertical dim zone distribution was concentrated within the buildups as they prograded to the basin margin (B).

The potential presence of hydrocarbon-charged fluids in the Browse Basin, when considered together with regional compression, provides a driving force for mud volcanism by decreasing mud density and increasing buoyancy forces (Hovland and Curzi, 1989; Brown, 1990; Rollet et al., 2009). Yet, questions remain as to the source of mud for the >20-m-high mud volcanoes in the Browse Basin. Examples of mud volcanoes from southwest Taiwan sit above mud diapirs (Brown, 1990; Milkov, 2000; Talukder et al., 2007). In the Browse Basin, mud volcanoes sit above a thick unit of hemipelagic sediment on the modern sea floor (Fig. 12A). Conversely, no mud diapirs are observed in the study area within pre-Miocene strata. Pinnacles observed above the Eocene–early Oligocene ramp, and within late Oligocene–Miocene isolated carbonate buildups, notably occur within porous and permeable facies (Wilson, 1975) and contain only a small percentage of mud (Figs. 3, 6, and 8).

Potential sources of mud could come from horizontal seismic reflections within isolated carbonate buildups, e.g., lagoonal muds (Bachtel et al., 2004). Alternatively, during transgressive periods, isolated carbonate buildups may have been onlapped by parallel, flat reflections, exhibiting low variance (Figs. 8, 9, and 10), suggesting they were draped by fine-grained basinal muds (Bachtel et al., 2004). These muds may also have provided a source of mud, or acted as a barrier to flow, against which pore fluid pressure was able to increase (Kalinko, 1964). This seems to contradict studies indicating that mud volcanoes do not form above carbonate strata (Margreth et al., 2011).

An alternative interpretation is that pinnacle features represent methane-derived carbonates (Hovland, 1990), as suggested for carbonate deposits at contemporary and ancient methane seeps (Fig. 14; Mullins and Neumann, 1979; Hovland et al., 1987, 1994; Hovland and Judd, 1988; O'Brien et al., 2003; Sumida et al., 2004; Reitner et al., 2005a, 2005b). Localized high-amplitude seismic reflections beneath isolated carbonate buildups and mounds (Figs. 6 and 12), often rooted on an erosional surface, are similar in character to carbonate-cemented hardgrounds in the Arafura Basin, Northwest Australia (Rollet et al., 2009). Also, pinnacle features in the study area are comparable in size and geometry to mounds up to 30 m high on the Yampi Shelf, interpreted as carbonate crusts associated with fluid flow (Rollet et al., 2009).

Carbon isotope data from the Brecknock-1 well (southern Browse Basin) record $\delta^{13}C$ values from 0.9‰ to 2.4‰ for the Miocene carbonate sequence (Rosleff-Soerensen et al., 2012), significantly lower than typical $\delta^{13}C$ values (up to +30‰) for methanogenic carbonates (Claypool

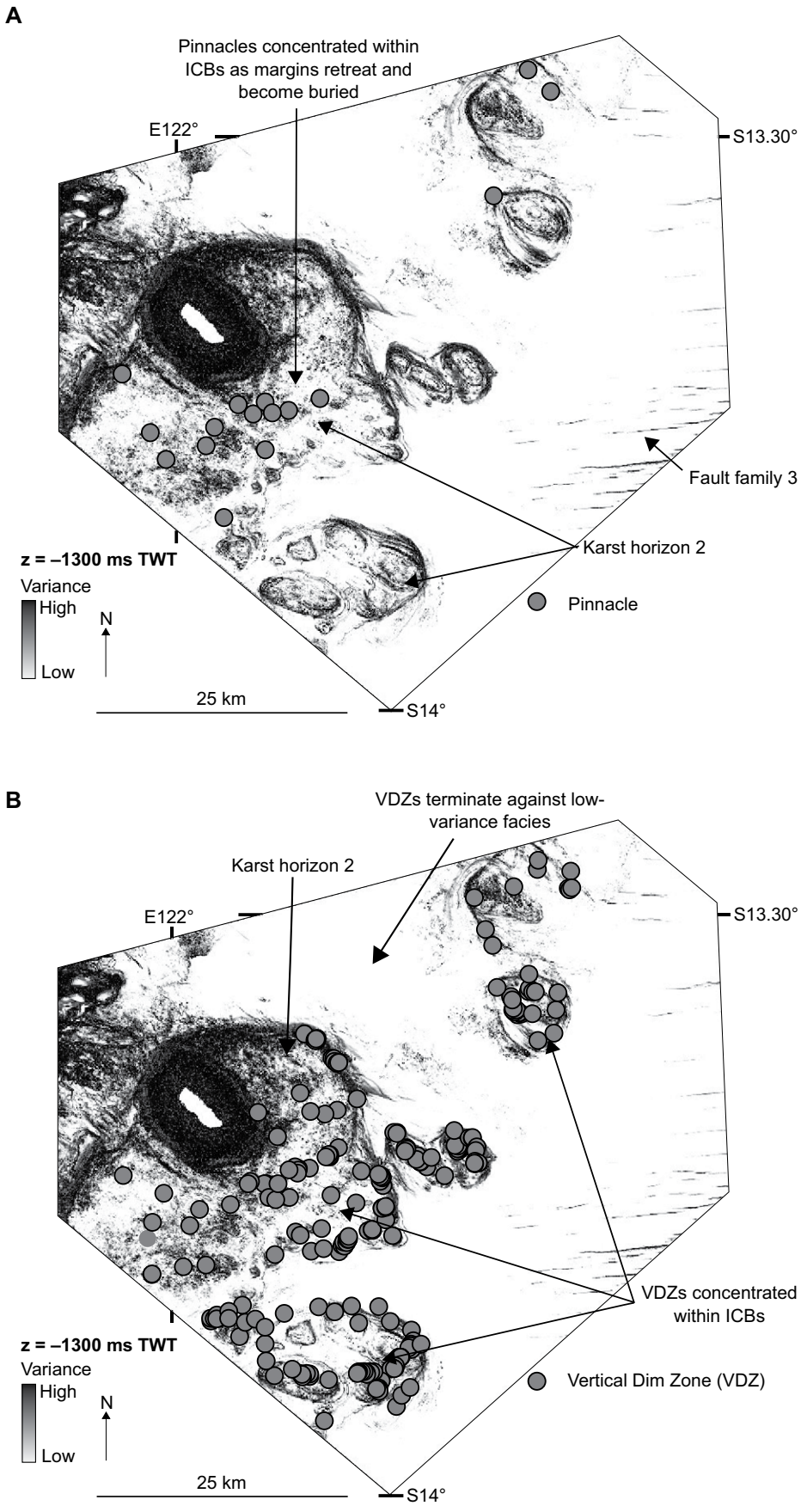

Figure 10. (A–B) Pair of variance slices taken at –1300 ms two-way time (TWT). The variance slices show the position of pinnacles (A) and corresponding vertical dim zones (VDZs; B). Pinnacles are concentrated within isolated carbonate buildup (ICB) interiors, but become scarcer. Pinnacles do not occur above low-variance strata, which buried the basin-margin barrier reef. Vertical dim zone distribution continued to be concentrated within isolated carbonate buildup interiors and above karsts. No vertical dim zones occur above low-variance strata, suggesting low-variance strata were acting as a seal.

and Kaplan, 1974; Naehr et al., 2000, 2007), but suggestive of precipitation from sea water (Naehr et al., 2000, 2007; Díaz-del-Río et al., 2003). Notwithstanding the latter interpretation, it is important to acknowledge that the Brecknock-1 well is located over 75 km to the southwest of the seismic volume (Fig. 1) and does not sample a pinnacle. The limited data available from the Brecknock-1 well are not conclusive.

A third explanation is that pinnacles represent the first seismically resolved patch reefs preceding the growth of the larger isolated carbonate buildups that characterize the late Oligocene–Miocene and, therefore, have no association with fluid flow. This would fit with the re-evaluation by Logan et al. (2010) of the data interpreted in O'Brien et al. (2003) for other parts of Northwest Australia. While pockmarks and mud volcanoes are observed on the present-day sea floor, the absence of pockmarks within the Upper Oligocene–Miocene sequence indicates fluid flow was not enough to drive mud volcano or methanogenic carbonate formation in the study area (Fig. 12). Alternatively, it can indicate that fluid flow postdated the Miocene. As such, the observed relationship between seismic anomalies and pinnacles may relate to velocity pull-ups caused by overlying isolated carbonate buildups, or by shallow faults or fractures with negligible offset (O'Brien et al., 2002; Logan et al., 2010), likely associated with regional Neogene compression (Jones et al., 2008).

Was There an Active Seep-Reef Relationship in the Browse Basin during the Miocene?

This study identifies no relationship between fault-generated topography and isolated carbonate buildup growth (Figs. 4 and 6), agreeing with Howarth and Alves (2016). Instead, we document a causal relationship between seismic anomalies and pinnacle features, which served

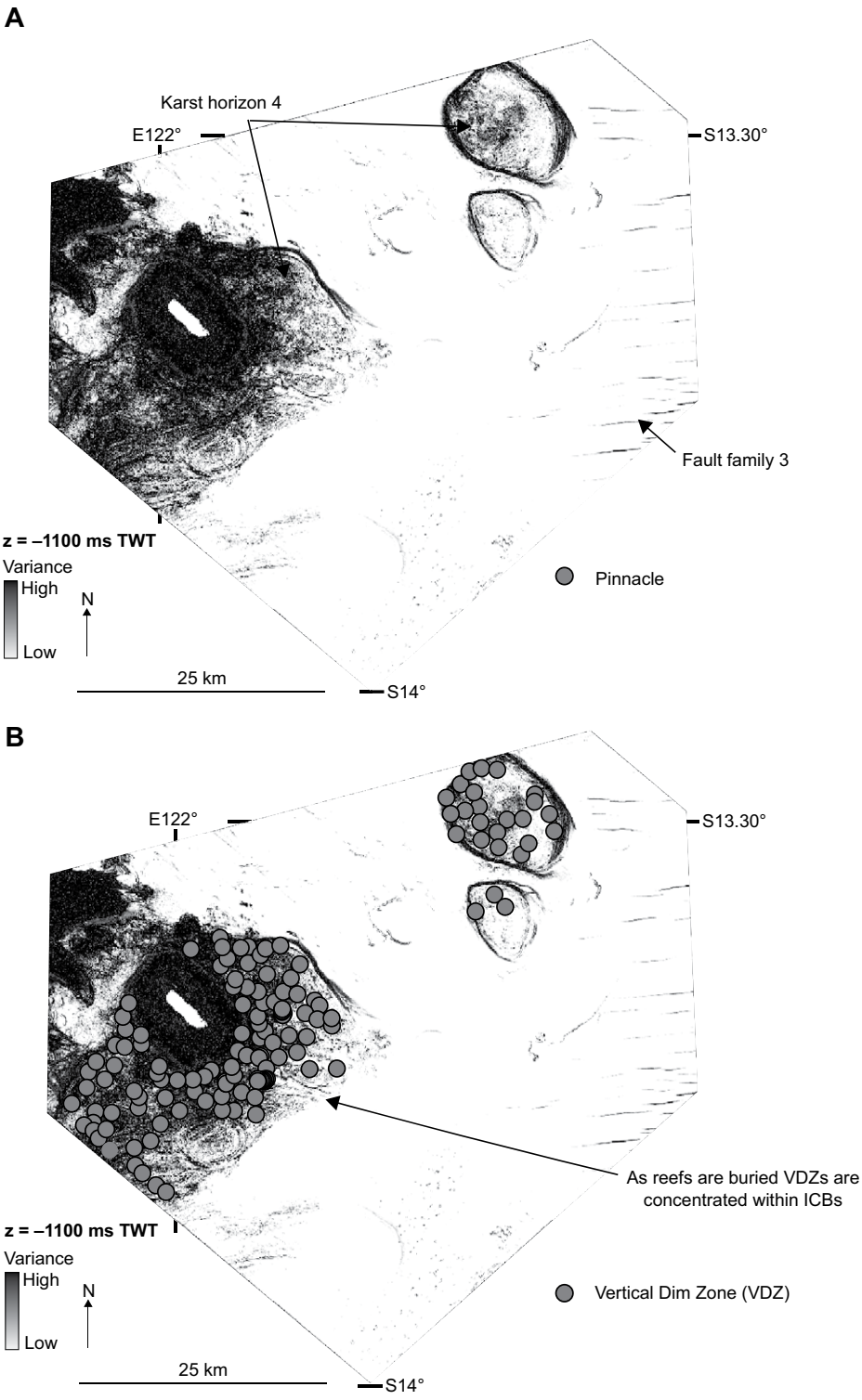

Figure 11. (A–B) Pair of variance slices taken at –1100 ms two-way time (TWT). The variance slices show the position of pinnacles (A) and corresponding vertical dim zones (VDZs; B). During the final phase of isolated carbonate buildup (ICB) growth, no pinnacles are observed (A). Position of the vertical dim zones mirrored the shrinking isolated carbonate buildups and was focused within buildup interiors (B). The scarcity of vertical dim zones within low-variance strata suggests they have good sealing potential. Consequently, vertical dim zone distribution was likely controlled by depositional facies distribution within the Eocene–early Oligocene ramp and late Oligocene–Miocene rimmed platform.

as focal points from which larger isolated carbonate buildups developed (Figs. 6 and 14). While Logan et al. (2010) dismissed a seep-reef relationship in other parts of Northwest Australia, upon integrating the results in this paper with regional tectonics (Macgregor, 1993) and data from the local petroleum system (O'Brien and Woods, 1995; Blevin et al., 1998a; Grosjean et al., 2016), we provide evidence to support the essentially Miocene migration of hydrocarbon-bearing fluids in the Browse Basin. This migration could have generated active seepage sites on the late Oligocene–Miocene paleo-seafloor to support the formation of mud volcanoes or methanogenic carbonates.

The absence of pockmarks within the Upper Oligocene–Miocene sequence, and other studies of seep-reef relationships in the Browse Basin (e.g., Logan et al., 2010), limits the interpretation of pinnacles as fluid-flow–related features. In fact, to determine whether seismic anomalies beneath pinnacle features are false or real structures, accurate acoustic logs are required from the intervals in which they occur to generate accurate velocity models (Marfurt and Alves, 2015), data that are not provided by the Poseidon-1 and Poseidon-2 wells. However, the data in this work show that the topography generated by the pinnacle features exceeds the minimum topography of 10 m required to trigger preferential isolated carbonate buildup growth (Figs. 5, 6, and 7; Rosleff-Soerensen et al., 2016). The observation that these features appear routinely at the base of isolated carbonate buildups (Figs. 3 and 6) suggests they were in place prior to the main phase of isolated carbonate buildup growth. The fact that not all pinnacle features developed larger isolated carbonate buildups above, particularly in the deeper parts of the basin and carbonate platform, is a proof that the topography generated by the pinnacles was not always sufficient to raise the sea floor into the photic zone, where reef-building organisms could eventually establish. It thus shows that pinnacles were capable of placing the sea floor in the photic zone only where the Browse Basin shelf was at its shallowest (Fig. 12).

Hence, the model favored in this paper is one in which hydrocarbon-bearing fluids from deeper reservoir intervals provided enough methane and sulfate to stimulate precipitation through anaerobic oxidation of methane below the sediment-water interface (Reitner et al., 2005a, 2005b; Han et al., 2008). As a result, precipitation of a bottom plate of hard sediment could have ensued, upon which "tower" or "mounded" methanogenic carbonates (Reitner et al., 2005a, 2005b; Rollet et al., 2009) generated the pinnacle features observed in the Upper Oligocene–Miocene sequence (Fig. 14). A limitation to

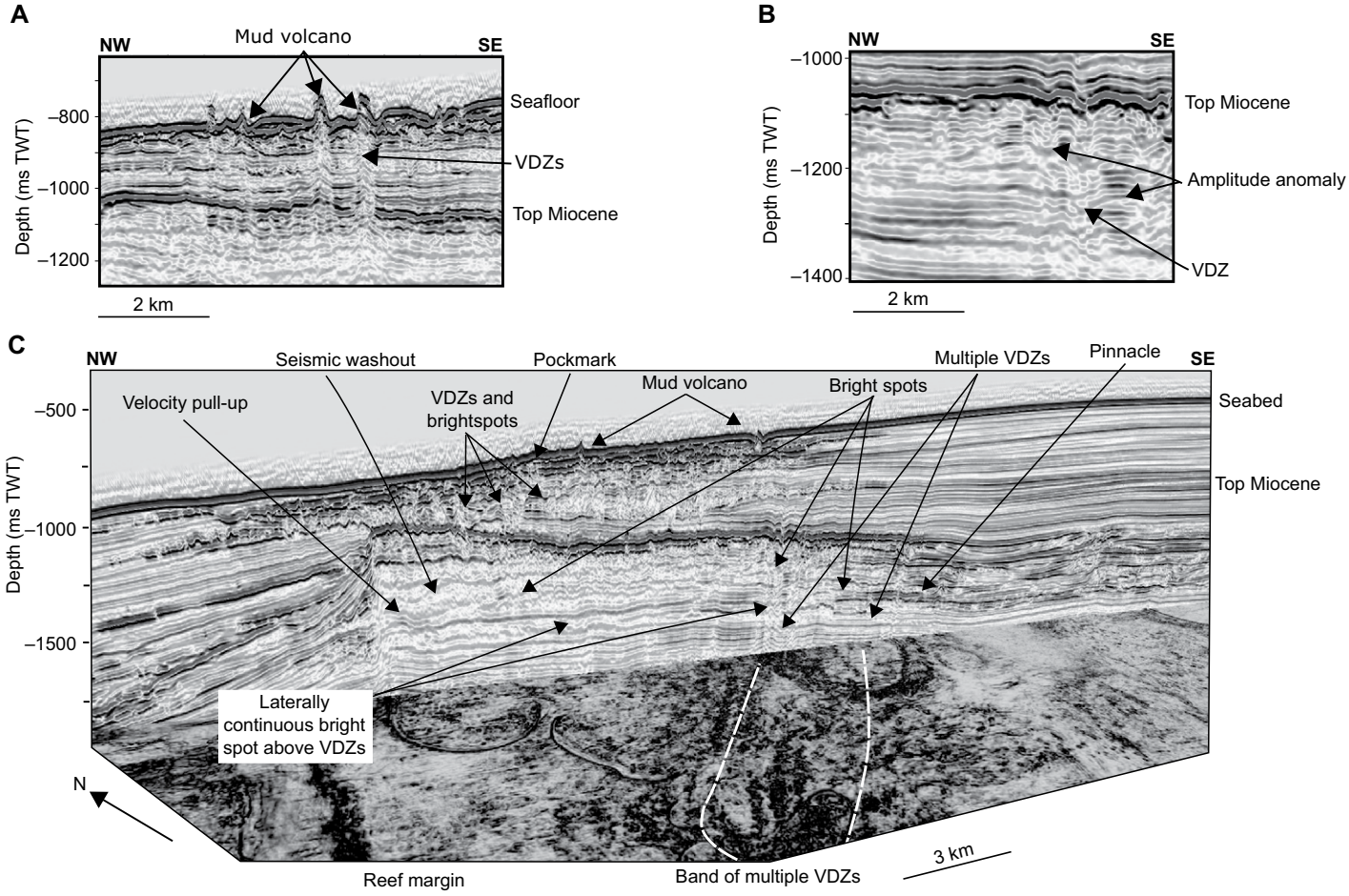

Figure 12. (A) Two-way time (TWT) seismic profile highlighting the presence of mud volcanoes on the present-day sea floor, above vertical dim zones. Considering that the present-day North West Shelf is a high-energy, shallow-water region that experiences macrotides, seasonal cyclonic storms, and long-period swells (James et al., 2004), the presence of mud volcanoes on the sea floor supports the idea that structures associated with seepage were not quickly destroyed in the late Oligocene–Miocene (Logan et al., 2010). The presence of mud volcanoes on the modern sea floor also suggests that their late Oligocene–Miocene counterparts had enough time to be colonized by reef-building organisms. (B) TWT seismic profile showing a number of interpreted bright spots close to interpreted vertical dim zones. (C) Interpreted TWT seismic profile and variance slice presenting a selection of seismic anomalies identified in the Browse Basin. Multiple vertical dim zones (VDZs) are observed within isolated carbonate buildups and form a northeast-trending zone across the study area. In addition, bright spots and a mud volcano are observed on the seismic line. Seismic washouts were identified on the northwest margin of the isolated carbonate buildup region and are common features inside the region of isolated carbonate buildups. These seismic washouts suggest active fluid accumulations and flow. Velocity pull-ups are also observed beneath the margins of isolated carbonate buildups.

this model is that methanogenic carbonates are commonly restricted to anoxic conditions (Peckmann et al., 2001), and planktonic assemblages from the Browse Basin indicate that the early Miocene platform experienced shallow, warm, and oxic conditions (Rosleff-Soerensen et al., 2012; Howarth and Alves, 2016). These conditions cause aerobic oxidation of methane and dissolution of methanogenic carbonates, rather than their precipitation (Teichert et al., 2005). Thus, for methanogenic carbonates to have formed in the Browse Basin, either: (1) stratification of the water column occurred during the late Oligocene–Miocene, allowing for the formation of anoxic bottom waters, or (2) communities of archaea and sulfate-reducing, bacteria-coated chemoherms protected them from oxic seawater conditions, and allowed methanogenic carbonate production within the underlying anoxic microenvironment. This same process has been proposed for methanogenic carbonates at Hydrate Ridge, offshore western North America (Teichert et al., 2005).

CONCLUSIONS

The main conclusions of this study are:

(1) Pre-Paleogene fault systems focused fluid flow from Mesozoic reservoirs into Paleogene strata. Above these reservoirs, depositional facies within prograding clinoforms of a Eocene–early Oligocene carbonate ramp and late Oligocene–Miocene isolated carbonate buildups controlled fluid flow in the study area.

(2) Seismic anomalies within Upper Oligocene–Miocene strata lead us to infer that fluid flow, and surface seepage of hydrocarbon-bearing fluids, was common on the paleo-seafloor of the Browse Basin.

(3) Pinnacle features can be interpreted as mud volcanoes, methanogenic carbonates, or the first patch reefs preceding the larger isolated carbonate buildups. Given the tectonic setting and evolution of the petroleum system in the study area, their association with fluid flow is not ruled out.

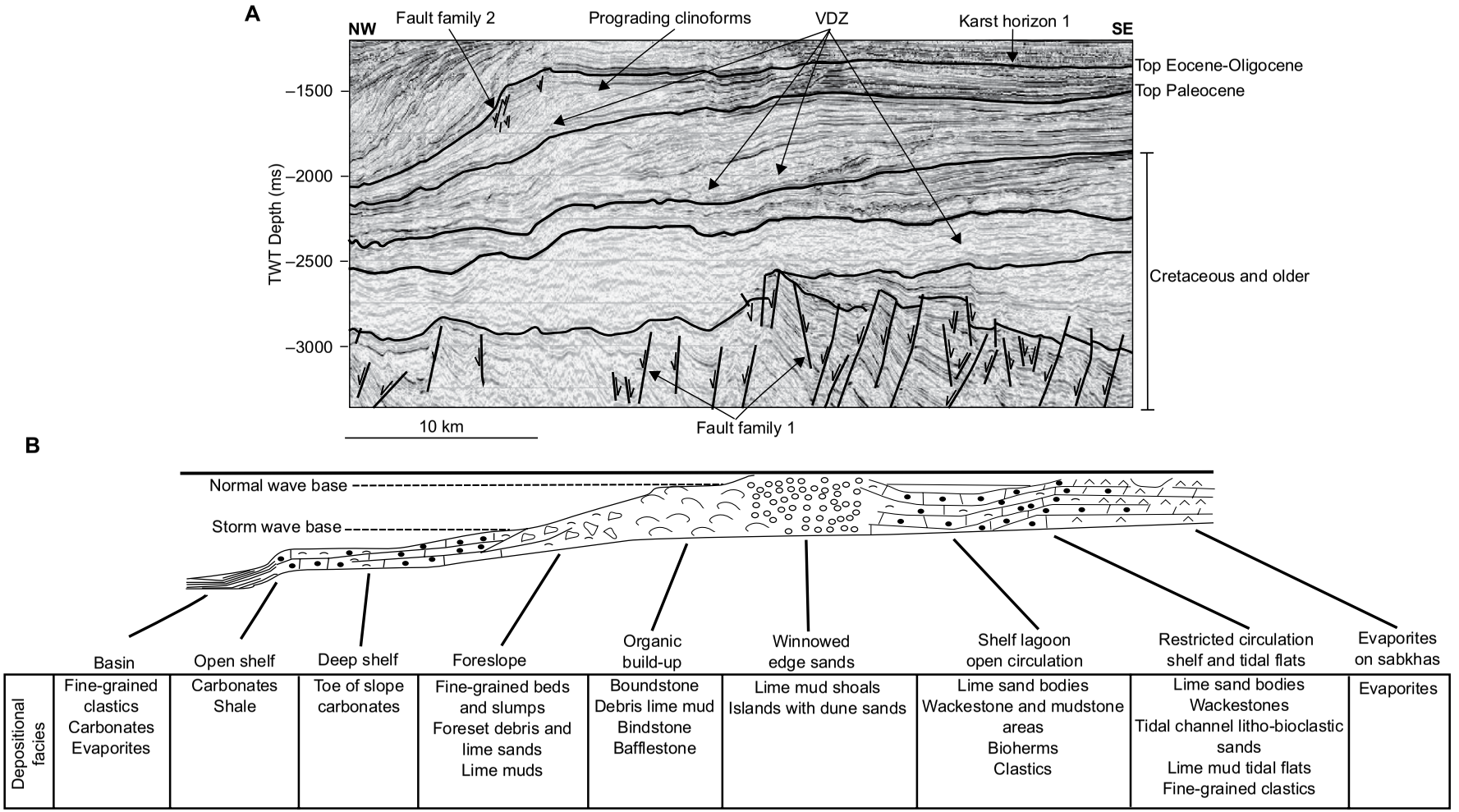

Figure 13. (A) Two-way time (TWT) seismic profile showing the Eocene–early Oligocene carbonate ramp, and (B) an idealized facies distribution for a carbonate ramp (after Wilson, 1975). Fluid-flow structures show good porosity and permeability. This indicates that the spatial distribution of fluid-flow features in the Upper Oligocene–Miocene sequence was controlled by the relative distribution of depositional facies on the underlying (Eocene–early Oligocene) carbonate ramp. VDZ—vertical dim zone.

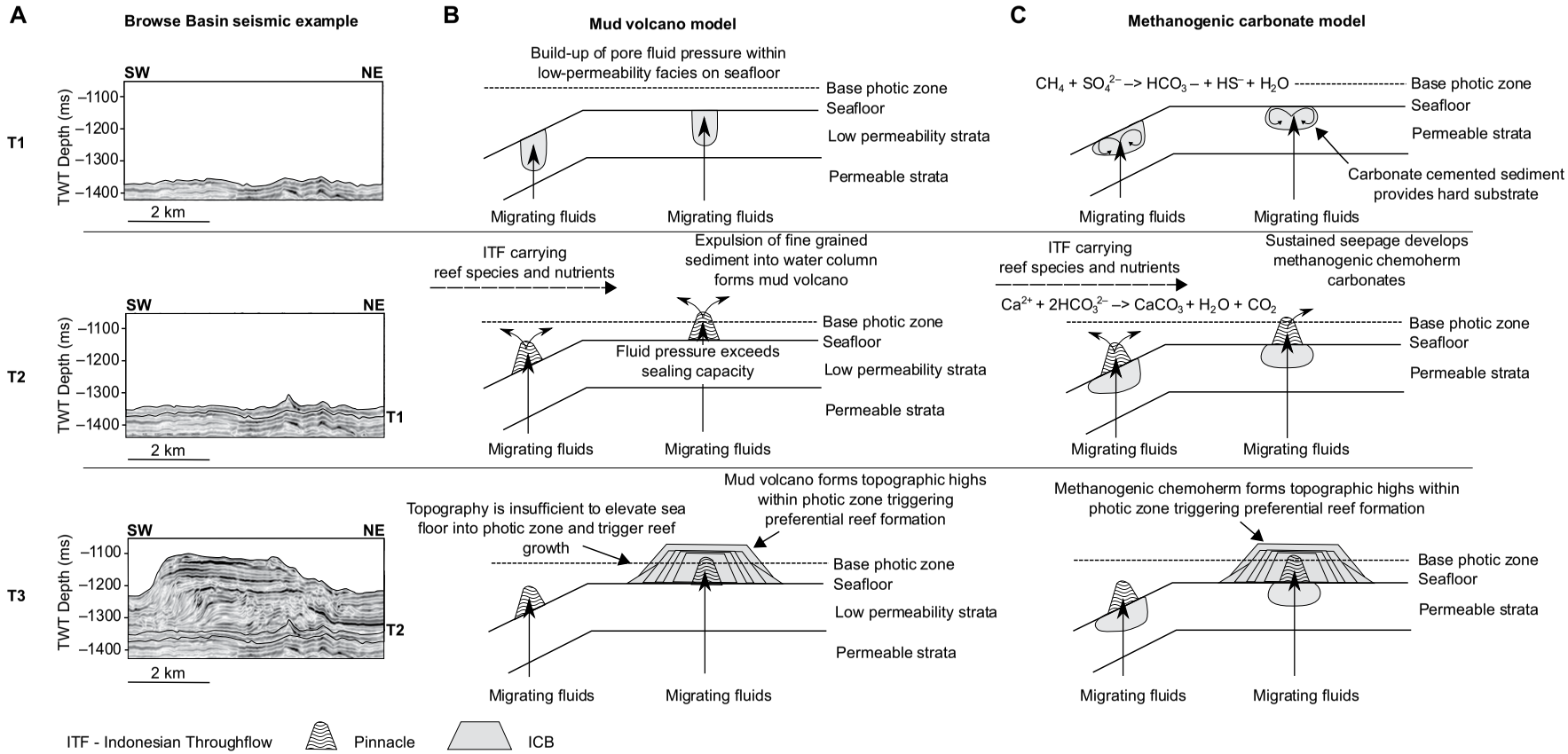

Figure 14. (A) Two-way time (TWT) seismic profile and (B–C) corresponding interpretation cartoons depicting the possible origin of pinnacles associated with fluid flow, and how they influenced isolated carbonate buildup (ICB) growth in the study area. The first interpretation (B) considers pinnacle features as mud mounds, while the second interpretation (C) invokes a methanogenic origin for these same pinnacles. After they were generated, pinnacles formed topographic highs on the sea floor that acted as focal points for isolated carbonate buildup–building organisms carried by ocean currents. Migrating fluid provided a source of nutrients for seafloor organisms. Whether a pinnacle feature developed a larger isolated carbonate buildup was determined by its height relative to the base of the photic zone, and if conditions below the photic zone were favorable (or not) for isolated carbonate buildup growth. This latter postulate explains why some of the pinnacle features in the Browse Basin did not develop larger isolated carbonate buildups above them.

(4) Based on the results in this work, and on the current understanding of the Browse Basin's carbonate system, pinnacles represent the first isolated patch reefs formed prior to the larger isolated carbonate buildups, with underlying seismic anomalies deriving from velocity pull-ups or small-scale fractures through which fluid was able to migrate.

(5) In the absence of fault-generated topography, pinnacles generated sufficient antecedent topography to trigger the preferential settlement of reef-building organisms, and thus controlled the distribution of isolated carbonate buildups in the Browse Basin.

ACKNOWLEDGMENTS

The work contained in this paper is part of a Ph.D. study supported by the Natural Environment Research Council (NERC) Centre for Doctoral Training (CDT) in Oil and Gas and cosponsored by Cardiff University. Geosciences Australia is acknowledged for the provision of data for this research paper. We acknowledge Schlumberger (Petrel©) for granting academic licenses to Cardiff's 3-D Seismic Laboratory. We thank the two anonymous reviewers and Cathy Hollis for their suggestions and improvements to initial versions of this work.

REFERENCES CITED

Ahr, W.M., 1973, The carbonate Ramp: An alternative to the shelf model: Gulf Coast Association of Geological Societies Transactions, v. 23, p. 221–225.

Aloisi, G., Bouloubassi, I., Heijs, S.K., Pancost, R.D., Pierre, C., Sinninghe Damsté, J.P., Gottschal, J.C., Forney, L.J., and Rouchy, J.-M., 2002, CH_4-consuming microorganisms and the formation of carbonate crusts at cold seeps: Earth and Planetary Science Letters, v. 203, p. 195–203, https://doi.org/10.1016/S0012-821X(02)00878-6.

Apthorpe, M., 1988, Cainozoic depositional history of the Northwest Shelf, *in* Purcell, P.G., and Purcell, R.R. eds., The Northwest Shelf, Australia: Proceedings of Petroleum Exploration Society of Western Australia Symposium: Perth, Western Australia, Petroleum Exploration Society of Australia, p. 55–84.

AGSO (Australia Geological Survey Organisation) North West Shelf Study Group, 1994, Deep reflections on the North West Shelf: Changing perceptions of basin formation, *in* Purcell, P.G., ed., The Sedimentary Basins of Western Australia: Perth, Proceedings of Petroleum Exploration Society of Australia Symposium, p. 63–76.

Bachtel, S.L., Kissling, R.D., Martono, D., Rahardjanto, S., Dunn, P.A., and MacDonald, B.A., 2004, Seismic stratigraphic evolution of the Miocene–Pliocene Segitiga Platform, East Natuna Sea, Indonesia: The origin, growth and demise of an isolated carbonate platform, *in* Eberli, G.P., Masaferro, J.L., and Sarg, J.F., eds., Seismic Imaging of Carbonate Reservoirs and Systems: American Association of Petroleum Geology Memoir 81, p. 309–328.

Bachtel, S.L., Posamentier, H.W., and Gerber, T.P., 2011, Seismic geomorphology and stratigraphic evolution of a Tertiary-aged isolated carbonate platform system, Browse Basin, Northwest Shelf of Australia—Part II, *in* Wood, L.J., Simo, T.T., and Rosen, N.C., eds., Seismic Imaging of Depositional and Geomorphic Systems: 30th Annual Gulf Coast Section Society for Sedimentary Geology (SEPM) Foundation Bob F. Perkins Research Conference (Houston, Texas, 5–8 December 2010): Red Hook, New York, Curran, p. 115–135.

Barber, A.J., Tjokrosapoetro, S., and Charlton, T.R., 1986, Mud volcanoes, shale diapirs, wrench faults and mélanges in accretionary complexes, eastern Indonesia: American Association of Petroleum Geologists Bulletin, v. 70, no. 11, p. 1729–1741.

Barber, T., and Brown, K., 1986, Mud diapirism: The origin of mélanges in accretionary complexes?: Geology Today, v. 4, no. 3, p. 89–94.

Belde, J., Back, S., Bourget, J., and Reuning, L., 2017, Oligocene and Miocene carbonate platform development in the Browse Basin, Australian Northwest Shelf: Journal of Sedimentary Research, v. 87, no. 8, p. 795–816, https://doi.org/10.2110/jsr.2017.44.

Blevin, J.E., Boreham, C.J., Summons, R.E., Struckmeyer, H.I.M., and Loutit, T.S., 1998a, An effective Lower Cretaceous petroleum system on the Northwest Shelf: Evidence from the Browse Basin, *in* Purcell, P.G., and Purcell, R.R., eds., The Sedimentary Basins of Western Australia 2: Proceedings of the Petroleum Exploration Society of Australia Symposium: Perth, Western Australia, Petroleum Exploration Society of Australia, p. 397–420.

Blevin, J.E., Struckmeyer, H.I.M., Cathro, D.L., Totterdell, J.M., Boreham, C.J., Romine, K.K., Loutit, T.S., and Sayers, J., 1998b, Tectonostratigraphic framework and petroleum systems of the Browse Basin, Northwest Shelf, *in* Purcell, P.G., and Purcell, R.R., eds., The Sedimentary Basins of Western Australia 2: Proceedings of the Petroleum Exploration Society of Australia Symposium: Perth, Western Australia, Petroleum Exploration Society of Australia, p. 369–395.

Brouwer, M.J.M., and Schwander, M.M., 1987, Passive margins: Cenozoic carbonate banks, Foz Do Amazonas Basin, northeastern Brazil, *in* Bally, A.W., ed., Atlas of Seismic Stratigraphy: American Association of Petroleum Geologists Studies in Geology 27, no. 2, p. 174–178.

Brown, K.M., 1990, The nature and hydrogeologic significance of mud diapirs and diatremes for accretionary systems: Journal of Geophysical Research, v. 95, p. 8969–8982, https://doi.org/10.1029/JB095iB06p08969.

Carrasco, V.B., 2003, Paleokarst in the marginal Cretaceous rocks, Gulf of Mexico, *in* Bartolini, C., Buffer, R.T., and Blickwelde, J., eds., The Circum–Gulf of Mexico and the Caribbean: Hydrocarbon Habitats, Basin Formation, and Plate Tectonics: American Association of Petroleum Geologists Memoir 79, p. 169–183.

Cartwright, J., 2007, The impact of 3D seismic data on the understanding of compaction, fluid flow and diagenesis in sedimentary basins: Journal of the Geological Society [London], v. 164, p. 881–893, https://doi.org/10.1144/0016-76492006-143.

Chen, S.-C., Hsu, S.-K., Wang, Y., Chung, S.-H., Chen, P.-C., Tsai, C.-H., Liu, C.-S., Lin, H.-S., and Lee, Y.-W., 2014, Distribution and characters of the mud diapirs and mud volcanoes off southwest Taiwan: Journal of Asian Earth Sciences, v. 92, p. 201–214, https://doi.org/10.1016/j.jseaes.2013.10.009.

Claypool, G.E., and Kaplan, I.R., 1974, The origin and distribution of methane in marine sediments, *in* Kaplan, I.R., ed., Natural Gases in Marine Sediments: New York, Plenum Press, p. 99–139, https://doi.org/10.1007/978-1-4684-2757-8_8.

Collins, L.B., 2010, Controls on morphology and growth history of coral build-ups of Australians western margin, *in* Morgan, W.A., George, A.D., Harris, P.M., Kupecz, J.A., and Sarg, J.F., eds., Cenozoic Carbonate Systems of Australia: Society of Sedimentary Geology (SEPM) Special Publication 95, p. 195–217.

Collon-Drouaillet, P., Henrion, V., and Pellerin, J., 2012, An algorithm for 3D simulation of branchwork karst networks using Horton parameters and an application to a synthetic case, *in* Garland, J., Neilson, J.E., Laubach, S.E., and Whidden, K.J., eds., Advances in Carbonate Exploration and Reservoir Analysis: Geological Society, London, Special Publication 370, p. 295–306, https://doi.org/10.1144/SP370.3.

ConocoPhillips, 2012, 2009 Poseidon 3D Marine Surface Seismic Survey: Interpretation Reports WA-315-P and AQ-398-P Browse Basin Western Australia: ConocoPhillips, 43 p.

Courgeon, S., Bourget, J., and Jorry, S.J., 2016, A Pliocene–Quaternary analogue for ancient epeiric carbonate settings: The Malita intra shelf basin (Bonaparte Basin, northwest Australia): American Association of Petroleum Geologists Bulletin, v. 100, p. 565–595, https://doi.org/10.1306/02011613196.

Díaz-del-Río, V., Somoza, L., Martínez-Frias, J., Mata, M.P., Delgado, A., Hernandez-Molina, F.J., Lunar, R., Martín-Rubí, J.A., Maestro, A., Fernández-Puga, M.C., León, R., Llave, E., Medialdea, T., and Vázquez, J.T., 2003, Vast fields of hydrocarbon-derived carbonate chimneys related to the accretionary wedge/olistostrome of the Gulf of Cádiz: Marine Geology, v. 195, p. 177–200, https://doi.org/10.1016/S0025-3227(02)00687-4.

Dimitrov, L.I., 2002, Mud-volcanoes—The most important pathway for degassing deeply buried sediments: Earth-Science Reviews, v. 59, p. 49–76, https://doi.org/10.1016/S0012-8252(02)00069-7.

Eberli, G.P., and Ginsburg, R.N., 1987, Segmentation and coalescence of Cenozoic carbonate platforms, northwester Great Bahama Bank: Geology, v. 15, p. 75–79, https://doi.org/10.1130/0091-7613(1987)15<75:SACOCC>2.0.CO;2.

Fathiyah Jamaludin, S.N., Latiff, A.H.A., and Kadir, A.A., 2015, Interpretation of gas seepage on seismic data: Example from Malaysian offshore: Journal of Physics: Conference Series, v. 660, p. 1–7, https://doi.org/10.1088/1742-6596/660/1/012002.

Field, M.S., 1999, A Lexicon of Cave and Karst Terminology with Special Reference to Environmental Karst Hydrology: U.S. Environmental Protection Agency National Centre for Environmental Assessment Report EPA/600/R-99/006, 201 p. (digital version by Karst Waters Institute).

Fournier, F., Borgomano, J., and Montaggioni, L.F., 2005, Development patterns and controlling factors of Tertiary carbonate build-ups: Insights from high-resolution 3D seismic and well data in the Malampaya gas field (offshore Palawan, Philippines): Sedimentary Geology, v. 175, p. 189–215, https://doi.org/10.1016/j.sedgeo.2005.01.009.

Fournillon, A., Abelard, S., Viseur, S., Arfib, B., and Borgomano, J., 2012, Characterization of karstic networks by automatic extraction of geometrical and topological parameters: Comparison between observations and stochastic simulations, *in* Garland, J., Neilson, J.E., Laubach, S.E., and Whidden, K.J., eds., Advances in Carbonate Exploration and Reservoir Analysis: Geological Society, London, Special Publication 370, p. 247–264, https://doi.org/10.1144/SP370.8.

Frazer, M., Whitaker, F., and Hollis, C., 2014, Fluid expulsion from over pressurised basins: Implications for Pb-Zn mineralisation and dolomitization of the East Midlands platform, northern England: Marine and Petroleum Geology, v. 55, p. 68–86, https://doi.org/10.1016/j.marpetgeo.2014.01.004.

Gallagher, S.J., Wallace, M.W., Li, C.L., Kinna, B., Bye, J.T., Akimoto, K., and Torii, M., 2009, Neogene history of the West Pacific Warm Pool, Kuroshio and Leeuwin Currents: Palaeoceanography, v. 24, PA1206, https://doi.org/10.1029/2008PA001660.

Gartrell, A., Zhang, Y., Lisk, M., and Dewhurst, D., 2003, Enhanced hydrocarbon leakage at fault intersections: An example from the Timor Sea, Northwest Shelf, Australia: Journal of Geochemical Exploration, v. 78–79, p. 361–365, https://doi.org/10.1016/S0375-6742(03)00125-0.

Ghosh, D., Abdul Halim, M.F., Brewer, M., Viratani, B., and Darman, N., 2010, Geophysical issues and challenges in Malay and adjacent basins from E & P perspective: The Leading Edge, v. 29, p. 436–449, https://doi.org/10.1190/1.3378307.

Grötsch, J., and Mercadier, C., 1999, Integrated 3D reservoir modeling based on 3D seismic: The Tertiary Malampaya and Camago build-ups, offshore Palawan, Philippines: American Association of Petroleum Geologists Bulletin, v. 83, p. 1703–1728.

Grosjean, E., Edwards, D.S., Kuske, T.J., Hall, L., Rollet, N., Zumbergem J., 2016, The source of oil and gas accumulations in the Browse Basin, Northwest Shelf of Australia: A geochemical assessment: American Association of Petroleum Geologists Search and Discovery article 10827.

Han, B.P., Liu, R.D., Luo, C.J., Yu, J.J., and Yu, L.S., 1998, Study on control of karstification to buried carbonate hill reservoir in Renqiu oilfield: Carsologica Sinica, v. 17, p. 75–80 [in Chinese with English abstract].

Han, X., Suess, E., Huang, Y., Bohrmann, G., Su, X., Eisenhauer, A., Rehder, G., and Fang, Y., 2008, Jiulong methane reef: Microbial mediation of seep carbonates in the South China Sea: Marine Geology, v. 249, p. 243–256, https://doi.org/10.1016/j.margeo.2007.11.012.

Harris, P.M., Frost, S.H., Seiglie, G.A., and Schneidermann, N., 1984, Regional unconformities and depositional cycles: Cretaceous of the Arabian Peninsula, *in* Schlee, J.S., ed., Interregional Unconformities and Hydrocarbon Accumulation: American Association of Petroleum Geologists Memoir 36, p. 67–80.

Harrowfield, M., and Keep, M., 2005, Tectonic modification of the Australian North-West Shelf: Episodic rejuvenation of long-lived basin divisions: Basin Research, v. 17, no. 2, p. 225–239, https://doi.org/10.1111/j.1365-2117.2005.00251.x.

Heward, A.P., Chuenbunchom, S., Maukel, G., Marsland, D., and Spring, L., 2000, Nang Nuan oil field, B6/27, Gulf of Thailand: Karst reservoirs of meteoric or deep-burial origin?: Petroleum Geoscience, v. 6, no. 1, p. 15–27, https://doi.org/10.1144/petgeo.6.1.15.

Ho, S., Cartwright, J.A., and Imbert, P., 2012, Vertical evolution of fluid venting structures in relation to gas flux, in the Neogene–Quaternary of the Lower Congo Basin, offshore Angola: Marine Geology, v. 332–334, p. 40–55, https://doi.org/10.1016/j.margeo.2012.08.011.

Hovland, M., 1990, Do carbonate build-ups form due to fluid seepage?: Terra Nova, v. 2, p. 8–18, https://doi.org/10.1111/j.1365-3121.1990.tb00031.x.

Hovland, M., and Curzi, P.V., 1989, Gas seepage and assumed mud diapirism in the Italian central Adriatic Sea: Marine and Petroleum Geology, v. 6, p. 161–169, https://doi.org/10.1016/0264-8172(89)90019-6.

Hovland, M., and Judd, A.G., 1988, Sea Bed Pockmarks and Seepages: Impact on Geology, Biology and the Marine Environment: London, Graham and Trotman Ltd., 293 p.

Hovland, M., Talbot, M.R., Qvale, H., Oulassen, S., and Aasberg, L., 1987, Methane-related carbonate cements in pockmarks of the North Sea: Journal of Sedimentary Petrology, v. 57, p. 881–892.

Hovland, M., Croker, P.F., and Martin, M., 1994, Fault-associated sea-bed mounds (carbonate knolls?) off western Ireland and north-west Australia: Marine and Petroleum Geology, v. 11, p. 232–246, https://doi.org/10.1016/0264-8172(94)90099-X.

Hovland, M., Jensen, S., and Fichler, C., 2012, Methane and minor oil macro-seep systems—Their complexity and environmental significance: Marine Geology, v. 332–334, p. 163–173, https://doi.org/10.1016/j.margeo.2012.02.014.

Howarth, V., and Alves, T.M., 2016, Fluid flow through carbonate platforms as evidence for deep-seated reservoirs in Northwest Australia: Marine Geology, v. 380, p. 17–43, https://doi.org/10.1016/j.margeo.2016.06.011.

James, N.P., Bone, Y., Kyser, T.K., Dix, G.R., and Collins, L.B., 2004, The importance of changing oceanography in controlling late Quaternary carbonate sedimentation on a high-energy, tropical oceanic ramp: Northwestern Australia: Sedimentology, v. 51, p. 1179–1205, https://doi.org/10.1111/j.1365-3091.2004.00666.x.

Jones, A.T., Kennard, J.M., Ryan, G.J., Bernardel, G., Earl, K., Rollet, N., Grosjean, E., and Logan, G.A., 2006, Geoscience Australia Marine Survey SS06/2006 Post-Survey Report: Natural Hydrocarbon Seepage Survey on the Ventral Northwest Shelf: Geoscience Australia, 693 p.

Judd, A.G., and Hovland, M., 2007, Sea Bed Fluid Flow: Cambridge, UK, Cambridge University Press, 475 p., https://doi.org/10.1017/CBO9780511535918.

Kalinko, M., 1964, Mud volcanoes, reasons of their origin, development and fading: All-Russia Petroleum Research Exploration Institute (VNIGRI) Transactions, v. 40, p. 30–54 [in Russian].

Keep, M., Bishop, A., and Longley, I., 2000, Neogene wrench reactivation of the Barcoo sub-basin, Northwest Australia: Implications for Neogene tectonics of the northern Australian margin: Petroleum Geoscience, v. 6, p. 211–220, https://doi.org/10.1144/petgeo.6.3.211.

Kerans, C., 1988, Karst-controlled reservoir heterogeneity in Ellenburger Group carbonates of west Texas: American Association of Petroleum Geologists Bulletin, v. 72, p. 1160–1183.

Kopf, A.J., 2002, Significance of mud volcanism: Reviews of Geophysics, v. 40, p. 2–52, https://doi.org/10.1029/2000RG000093.

Kroos, B.M., and Leythaeuser, D., 1996, Molecular diffusion of light hydrocarbons in sedimentary rocks and its role in migration and dissipation of natural gas, *in* Schumacher, D., and Abrams, M., eds., Hydrocarbon Migration and its Near-Surface Expression: American Association of Petroleum Geologists Memoir 66, p. 173–185.

Kuhnt, W., Holbourn, A., Hall, R., Zuvela, M., and Käse, R., 2004, Neogene history of the Indonesian throughflow, *in* Clift, P., Wang, P., Kuhnt, W., and Hayes, D., eds., Continent-Ocean Interactions within East Asian Marginal Seas: American Geophysical Union Geophysical Monograph 149, p. 299–320, https://doi.org/10.1029/149GM16.

Langhi, L., and Borel, G.D., 2008, Reverse structures in accommodation zone and early compartmentalization of extension system, Laminaria High (Northwest Shelf, Australia): Marine and Petroleum Geology, v. 25, p. 791–803, https://doi.org/10.1016/j.marpetgeo.2008.04.007.

Lindsay, R.F., Cantrell, D.L., Hughes, G.W., Keith, T.H., Mueller, H.W., III, and Russell, S.D., 2006, Ghawar Arab-D reservoir: Widespread porosity in shoaling-upward carbonate cycles, Saudi Arabia, *in* Harris, P.M., and Weber, L.J., eds., Giant Hydrocarbon Reservoirs of the World: From Rocks to Reservoir Characterization and Modeling: American Association of Petroleum Geologists Memoir 88, p. 97–137.

Liu, J.J., Liu, H.R., Tan, L., and Zhang, C.L., 2004, Reservoir characteristics and distributions of the Ordovician buried hill reservoir in Lunnan, Tarim Basin: Chinese Journal of Geology, v. 39, p. 532–542 [in Chinese with English abstract].

Logan, G.A., Jones, A.T., Kennard, J.M., Ryan, G.J., and Rollet, N., 2010, Australian offshore natural hydrocarbon seepage studies, a review and re-evaluation: Marine and Petroleum Geology, v. 27, p. 26–45, https://doi.org/10.1016/j.marpetgeo.2009.07.002.

Longley, I.M., Buessenschuett, C., Clydsdale, L., Cubitt, C.J., Davis, R.C., Johnson, M.K., Marshall, N.M., Murray, A.P., Somerville, R., Spry, T.B., and Thompson, N.B., 2002, The Northwest Shelf of Australia—Aa Woodside perspective, *in* Purcell, P.G., and Purcell, R.R., eds., The Sedimentary Basins of Western Australia: Proceedings of the Petroleum Exploration Society of Australia 3: Perth, Western Australia, Petroleum Exploration Society of Australia, p. 27–88.

Løseth, H., Gading, M., and Wensaas, L., 2009, Hydrocarbon leakage interpreted on seismic data: Marine and Petroleum Geology, v. 26, p. 1304–1319, https://doi.org/10.1016/j.marpetgeo.2008.09.008.

Loucks, R.G., 1999, Paleocave carbonate reservoirs; origins, burial-depth modifications, spatial complexity, and reservoir implications: American Association of Petroleum Geologists Bulletin, v. 83, p. 1795–1834.

Loucks, R.G., and Anderson, J.H., 1985, Depositional facies, diagenetic terrains, and porosity development in Lower Ordovician Ellenburger Dolomite, Puckett Field, west Texas, *in* Roehl, P.O., and Choquette, P.W., eds., Carbonate Petroleum Reservoirs: New York, Springer-Verlag, p. 19–38, https://doi.org/10.1007/978-1-4612-5040-1_2.

Macgregor, D., 1993, Relationships between seepage, tectonics and subsurface petroleum reserves: Marine and Petroleum Geology, v. 10, p. 606–619, https://doi.org/10.1016/0264-8172(93)90063-X.

Marfurt, K.J., and Alves, T.M., 2015, Pitfalls and limitations in seismic attribute interpretation of tectonic features: Interpretation (Tulsa), v. 3, no. 1, p. SB5–SB15, https://doi.org/10.1190/INT-2014-0122.1.

Margreth, S., Gennari, G., Ruggeberg, A., Comas, M.C., Pinheiro, L.M., and Spezzaferri, S., 2011, Growth and demise of cold-water coral exosystems on mud volcanoes in the West Alboran Sea: The messages from the planktonic and benthic foraminifera: Marine Geology, v. 281, p. 1–2, p. 26–39.

McGowran, B., Li, Q., Cann, J., Padley, D., McKirdy, D.M., and Shafik, S., 1997, Biogeographic impact of the Leeuwin Current in southern Australia since the late Middle Eocene: Palaeogeography, Palaeoclimatology, Palaeoecology, v. 136, p. 19–40, https://doi.org/10.1016/S0031-0182(97)00073-4.

McGowran, B., Holdgate, G.R., Li, Q., and Gallagher, S.J., 2004, Cenozoic stratigraphic succession in southeastern Australia: Australian Journal of Earth Sciences, v. 51, p. 459–496, https://doi.org/10.1111/j.1400-0952.2004.01078.x.

Michaelis, W., Seifert, R., Nauhaus, K., Treude, T., Thiel, V., Blumenberg, M., Knittel, K., Gieseke, A., Peterknecht, K., Pape, T., Boetius, A., Amann, R., Jørgensen, B.B., Widdel, F., Peckmann, J., Pimenov, N.V., and Gulin, M.B., 2002, Microbial build-ups in the Black Sea fueled by anaerobic oxidation of methane: Science, v. 297, p. 1013–1015, https://doi.org/10.1126/science.1072502.

Milkov, A.V., 2000, Worldwide distribution of submarine mud volcanoes and associated gas hydrates: Marine Geology, v. 167, p. 29–42, https://doi.org/10.1016/S0025-3227(00)00022-0.

Moss, J.L., and Cartwright, J., 2010, 3D seismic expression of km-scale fluid escape pipes from offshore Namibia: Basin Research, v. 22, p. 481–501, https://doi.org/10.1111/j.1365-2117.2010.00461.x.

Mullins, H.T., and Neumann, A.C., 1979, Deep carbonate bank margin structure and sedimentation in the northern Bahamas, *in* Doyle, L.J., and Pilkey, O.H., eds., Geology of Continental Slopes: Society of Economic Paleontologists and Mineralogists (SEPM) Special Publication 27, p. 165–192, https://doi.org/10.2110/pec.79.27.0165.

Naehr, T.H., Rodriguez, N.M., Bohrmann, G., Paull, C.K., and Botz, R., 2000, Methane-derived authigenic carbonates associated with gas hydrate decomposition and fluid venting above the Blake Ridge Diapir, *in* Paull, C.K., Matsumoto, R., Wallace, P.J., and Dillon, W.P., et al., Proceedings of the Ocean Drilling Program, Scientific Results: College Station, Texas, Ocean Drilling Program, v. 164, p. 285–300.

Naehr, T.H., Eichhubl, P., Orphan, V.J., Hovland, M., Paull, C.K., Ussler, W., III, Lorenson, T.D., and Greene, H.G., 2007, Authigenic carbonate formation at hydrocarbon seeps in continental margin sediments: A comparative study: Deep-Sea Research, Part II, Topical Studies in Oceanography, v. 54, p. 1268–1291, https://doi.org/10.1016/j.dsr2.2007.04.010.

O'Brien, G.W., and Woods, E.P., 1995, Hydrocarbon-related diagenetic zones (HRDZs) in the Vulcan Sub-basin, Timor Sea: Recognition and exploration implications: Australian Petroleum Production and Exploration Association (APPEA) Journal, v. 35, p. 220–252, https://doi.org/10.1071/AJ94015.

O'Brien, G.W., Glenn, K., Lawrence, G., Williams, A., Webster, M., Burns, S., and Cowley, R., 2002, Influence of hydrocarbon migration and seepage on benthic communities in the Timor Sea, Australia: Australian Petroleum Production and Exploration Association (APPEA) Journal, v. 42, p. 225–240, https://doi.org/10.1071/AJ01013.

O'Brien, G.W., Cowley, R., Lawrence, G., Williams, A., Webster, M., Tingate, P., and Burns, S., 2003, Migration, leakage and seepage characteristics of the offshore Canning Basin and Northern Carnarvon Basin: Implications for hydrocarbon prospectivity: Australian Petroleum Production and Exploration Association (APPEA) Journal, v. 43, p. 149–166, https://doi.org/10.1071/AJ02072.

O'Brien, G.W., Lawrence, G.M., Williams, A.K., Glenn, K., Barrett, A.G., Lech, M., Edwards, D.S., Cowley, R., Boreham, C.J., and Summons, R.E., 2005, Yampi Shelf, Browse Basin, North-West Shelf, Australia: A test-bed for constraining hydrocarbon migration and seepage rates using combinations of 2D and 3D seismic data and multiple, independent remote sensing technologies: Marine and Petroleum Geology, v. 22,

p. 517–549, https://doi.org/10.1016/j.marpetgeo.2004.10.027.

Omosanya, K.O., and Alves, T.M., 2013, A 3-dimensional seismic method to assess the provenance of mass-transport deposits (MTDs) on salt-rich continental slopes (Espirito Santo Basin, SE Brazil): Marine and Petroleum Geology, v. 44, p. 223–239, https://doi.org/10.1016/j.marpetgeo.2013.02.006.

Orange, D.L., 1990, Criteria helpful in recognizing shear-zone and diapiric mélanges, examples from the Hoh accretionary complex, Olympic Peninsula, Washington: Geological Society of America Bulletin, v. 102, p. 935–951, https://doi.org/10.1130/0016-7606(1990)102<0935:CHIRSZ>2.3.CO;2.

Osborne, M.J., and Swarbrick, R.E., 1997, Mechanisms for generating overpressure in sedimentary basins: A reevaluation: American Association of Petroleum Geologists Bulletin, v. 81, no. 6, p. 1023–1041.

Peckmann, J., Reimer, A., Luth, U., Luth, C., Hansen, B.T., Hei-Nicke, C., Hoefs, J., and Reitner, J., 2001, Methane-derived carbonates and authigenic pyrite from the northwestern Black Sea: Marine Geology, v. 177, p. 129–150, https://doi.org/10.1016/S0025-3227(01)00128-1.

Pickering, K.T., Agar, S.M., and Ogawa, T., 1988, Genesis and deformation of mud injections containing chaotic basalt limestone chert associations: Examples from the southwest Japan forearc: Geology, v. 16, p. 881–885, https://doi.org/10.1130/0091-7613(1988)016<0881:GADOMI>2.3.CO;2.

Pomar, L., 2001, Types of carbonate platforms: A genetic approach: Basin Research, v. 13, p. 313–334, https://doi.org/10.1046/j.0950-091x.2001.00152.x.

Rankey, E.C., 2017, Seismic architecture and seismic geomorphology of heterozoan carbonates: Eocene–Oligocene, Browse Basin, Northwest Shelf, Australia: Marine and Petroleum Geology, v. 82, p. 424–443, https://doi.org/10.1016/j.marpetgeo.2017.02.011.

Read, J.F., 1985, Carbonate platform facies models: American Association of Petroleum Geologists Bulletin, v. 69, p. 1–21.

Reitner, J., Peckmann, J., Blumenberg, M., Michaelis, W., Reimer, A., and Thiel, V., 2005a, Concretionary methane-seep carbonates and associated microbial communities in Black Sea sediments: Palaeogeography, Palaeoclimatology, Palaeoecology, v. 227, p. 18–30, https://doi.org/10.1016/j.palaeo.2005.04.033.

Reitner, J., Peckmann, J., Reimer, A., Schumann, G., and Thiel, V., 2005b, Methane-derived carbonate build-up and associated microbial communities at cold seeps on the lower Crimean shelf (Black Sea): Facies, v. 51, p. 66–79, https://doi.org/10.1007/s10347-005-0059-4.

Roberts, H.H., Aharon, P., and Walsh, M.M., 1993, Cold-seep carbonates of the Louisiana continental slope-to-basin floor, *in* Rezal, R., and Lavoie, D.L., eds., Carbonate Microfabrics: Berlin, Springer-Verlag, p. 95–104, https://doi.org/10.1007/978-1-4684-9421-1_7.

Rogers, J.N., Kelley, J.T., Belknap, D.F., Gontz, A., and Barnhardt, W.A., 2006, Shallow water pockmark formation in temperate estuaries: A consideration of origins in the western Gulf of Maine with special focus on Belfast Bay: Marine Geology, v. 225, p. 45–62, https://doi.org/10.1016/j.margeo.2005.07.011.

Rollet, N., Logan, G.A., Ryan, G., Judd, A.G., Totterdell, J.M., Glenn, K., Jones, A.T., Kroh, F., Struckmeyer, H.I.M., Kennard, J.M., and Earl, K.L., 2009, Shallow gas and fluid migration in the northern Arafura Sea (offshore northern Australia): Marine and Petroleum Geology, v. 26, p. 129–147, https://doi.org/10.1016/j.marpetgeo.2007.07.010.

Rosleff-Soerensen, B., Reuning, L., Back, S., and Kukla, P., 2012, Seismic geomorphology and growth architecture of a Miocene barrier reef, Browse Basin, NW-Australia: Marine and Petroleum Geology, v. 29, p. 233–254, https://doi.org/10.1016/j.marpetgeo.2010.11.001.

Rosleff-Soerensen, B., Reuning, L., Back, S., and Kukla, P., 2016, The response of a basin-scale Miocene barrier reef system to long-term, strong subsidence on a passive continental margin, Barcoo Sub-basin, Australian Northwest Shelf: Basin Research, v. 28, p. 103–123, https://doi.org/10.1111/bre.12100.

Saqab, M.M., and Bourget, J., 2015, Controls on the distribution and growth of isolated carbonate build-ups in the Timor Sea (NW Australia) during the Quaternary: Marine and Petroleum Geology, v. 62, p. 123–143, https://doi.org/10.1016/j.marpetgeo.2015.01.014.

Schroot, B.M., Klaver, G.T., and Schuttenhelm, R.T.E., 2005, Surface and subsurface expressions of gas seepage to the sea bed—Examples from the southern North Sea: Marine and Petroleum Geology, v. 22, p. 499–515, https://doi.org/10.1016/j.marpetgeo.2004.08.007.

Serié, C., Huuse, M., Schødt, N.H., Brooks, J.M., and Williams, A., 2016, Subsurface fluid flow in the deep-water Kwanza Basin, offshore Angola: Basin Research, v. 29, p. 1–31.

Somoza, L., Diaz-del-Rio, V., Leon, R., Ivanov, M., Fernandez-Puga, M.C., Gardner, J.M., Hernandez-Molina, F.J., Pinheiro, L.M., Roder, J., Lobato, A., Maestro, A., Vazquez, J.T., Medialdea, T., and Fernandez-Salas, L.M., 2003, Sea bed morphology and hydrocarbon seepage in the Gulf of Cádiz mud volcano area: Acoustic imagery, multibeam and ultra-high resolution seismic data: Marine Geology, v. 195, p. 153–176, https://doi.org/10.1016/S0025-3227(02)00686-2.

Stephenson, A.E., and Cadman, S.J., 1994, Browse Basin, northwest Australia: The evolution, paleogeography and petroleum potential of a passive continental margin: Palaeogeography, Palaeoclimatology, Palaeoecology, v. 111, p. 337–366, https://doi.org/10.1016/0031-0182(94)90071-X.

Struckmeyer, H.I.M., Blevin, J.E., Sayers, J., Totterdell, J.M., Baxter, K., and Cathro, D.L., 1998, Structural evolution of the Browse Basin, Northwest Shelf: New concepts from deep-seismic data, *in* Purcell, P.G., and Purcell, R.R., eds., The Sedimentary Basins of Western Australia 2: Proceedings of the Petroleum Exploration Society of Australia Symposium, Perth, Western Australia, Petroleum Exploration Society of Australia, p. 345–367.

Sumida, P.Y.G., Yoshinaga, M.Y., Madureira, L.A.S.-P., and Hovland, M., 2004, Sea bed pockmarks associated with deep-water corals off SE Brazilian continental slope, Santos Basin: Marine Geology, v. 207, p. 159–167, https://doi.org/10.1016/j.margeo.2004.03.006.

Talukder, A.R., Bialas, J., Klaeschen, D., Buerk, D., Brueckmann, W., Reston, T., and Breitzke, M., 2007, High-resolution, deep tow, multichannel seismic and sidescan sonar survey of the submarine mounds and associated BSR off Nicaragua Pacific margin: Marine Geology, v. 241, p. 33–43, https://doi.org/10.1016/j.margeo.2007.03.002.

Teichert, B.M.A., Bohrmann, G., and Suess, E., 2005, Chemoherms on Hydrate Ridge—Unique microbially-mediated carbonate build-ups growing into the water column: Palaeogeography, Palaeoclimatology, Palaeoecology, v. 227, no. 1-3, p. 67–85, https://doi.org/10.1016/j.palaeo.2005.04.029.

Tovaglieri, F., and George, A.D., 2014, Stratigraphic architecture of an Early-Middle Jurassic tidally influenced deltaic system (Plover Formation), Browse Basin, Australian Northwest Shelf: Marine and Petroleum Geology, v. 49, p. 59–83, https://doi.org/10.1016/j.marpetgeo.2013.09.011.

Veevers, J.J., and Cotteril, D., 1978, Western margin of Australia: Evolution of a rifted arch system: Geological Society of America Bulletin, v. 89, p. 337–355, https://doi.org/10.1130/0016-7606(1978)89<337:WMOAEO>2.0.CO;2.

Veevers, J.J., and Powell, C.McA., 1984, Dextral shear within the eastern Indo-Australian plate, *in* Veevers, J.J., ed., Phanerozoic Earth History of Australia: Oxford, UK, Clarendon Press, p. 102–103.

Wild, C., Rixen, T., Sánchez-Noguera, C., Merico, A., Jiménez, C., Cortés, J., and Naumann, M.S., 2015, A carbonate platform associated with shallow cold methane seeps in Golfo Dulce: Pacific Costa Rica: Galaxea: Journal of Coral Reef Studies, v. 17, p. 13–14, https://doi.org/10.3755/galaxea.17.13.

Wilson, J.L., 1975, Carbonate Facies in Geologic History: New York, Springer Verlag, 375 p., https://doi.org/10.1007/978-1-4612-6383-8.

Wilson, M.E.J., Bosence, D.W.J., and Limbong, A., 2000, Tertiary syntectonic carbonate platform development in Indonesia: Sedimentology, v. 47, p. 395–419, https://doi.org/10.1046/j.1365-3091.2000.00299.x.

Wright, V.P., Baceta, J.I., and Lapointe, P.A., 2014, Paleokarstic macroporosity development at platform margins: Lessons from the Paleocene of north Spain: Interpretation (Tulsa), v. 2, no. 3, p. SF1–SF16, https://doi.org/10.1190/INT-2013-0175.1.

Zhu, Z.R., Wyrwoll, K.H., Collins, L.B., Chen, J.H., Wasserburg, G.J., and Eisenhauer, A., 1993, High-precision U-series dating of Last Interglacial events by mass spectrometry: Houtman Abolhos Islands, Western Australia: Earth and Planetary Science Letters, v. 118, p. 281–293, https://doi.org/10.1016/0012-821X(93)90173-7.

Science Editor: Bradley S. Singer
Associate Editor: Ganqing Jiang

Manuscript Received 8 May 2017
Revised Manuscript Received 10 January 2018
Manuscript Accepted 26 February 2018

Printed in the USA